Optimal Two-Way Buffer-Aided Relaying: Achieving the Best Outage and Delay Performance with Small Buffer Sizes

Chadi Abou-Rjeily, *Senior Member IEEE*

***Abstract*—In this paper, we consider two-way relaying where two users exchange information through a decode-and-forward (DF) buffer-aided (BA) relay. We formulate a generic BA relaying protocol that is based on both the channel and buffer states and that can be parameterized by two parameters. Through a Markov chain analysis, we show how these parameters can be selected for the sake of minimizing the outage probability (OP) and average packet delay (APD) for asymptotic values of the signal-to-noise ratio. The performed optimization sheds more light on the impact of the buffer sizes on the triad of diversity order, coding gain and APD that can be contemplated. In particular, we prove that equipping the relay with two buffers of size three each is sufficient for extracting the full capabilities of two-way BA relaying. Depending on the network setup, one or both buffer sizes can be further reduced to two at the expense of a reduced coding gain without affecting the diversity order and asymptotic APD. Simulations under the generalized $\kappa-\mu$ fading demonstrate the appropriateness of the performed optimization of the relaying parameters and buffer sizes.**

***Index Terms*—Relaying, cooperation, decode-and-forward, buffer, data queue, Markov chain, outage probability, queuing delay, asymptotic analysis, diversity order.**

I. Introduction

The last years have witnessed an unprecedented progress in the area of buffer-aided (BA) relaying. Equipping the relays with buffers offers flexible scheduling that manifests into enhanced levels of throughput and diversity [1], [2]. BA relaying was primarily introduced in dual-hop one-way cooperative networks where the information is transferred from a source node to a destination node via a number of relays [1]–[9]. In the context of one-way relaying, research focused on the problem of relay selection in half-duplex (HD) decode-and-forward (DF) networks [3]–[5]. In [3], it has been demonstrated that activating the link with the highest instantaneous signal-to-noise ratio (SNR) achieves the full diversity order with infinitely large buffer sizes. By giving preference to transmission at the relays, the protocol in [4] resulted in reduced delays compared to [3]. By taking into account both the channel quality and buffer state, the BA scheme in [5] achieves full diversity with finite size buffers while keeping the delay at acceptable levels. The heuristic algorithms in [3]–[5] were unified in [6] in the special case of a single relay highlighting on the tradeoffs that can be achieved between the outage probability (OP) and average packet delay (APD). DF BA relaying with a single relay was considered in [7] with the objective of maximizing the throughput over a communication session that extends over an infinite number of time slots. While the one-way BA relaying schemes in [1]–[7] are deterministic, probabilistic schemes were proposed in [8], [9] where an additional randomness is imposed on the link selection protocol for the sake of achieving different levels of tradeoff between OP and APD.

In addition to one-way BA relaying, two-way BA relaying was also extensively studied due to its high spectral efficiency where two HD users exchange information via a relay [10]–[21]. Unlike one-way relaying where only the traffic generated by a source node (S) is considered, two-way relaying must also account for the traffic generated by the destination node (D). As such, unlike one-way BA selection protocols that select among two possible transmission modes (S transmits to a relay or a relay transmits to D) [1]–[9], two-way relaying involves an additional transmission mode where D transmits to a relay. Moreover, in two-way relaying, the relay transmits a XORed packet to both users in a broadcast phase. Finally, for one-way BA relaying, each relay is equipped with a single buffer for storing the information received from S. However, two-way BA relaying necessitates equipping each relay with two buffers (or, equivalently, splitting the single buffer into two disjoint parts) for the sake of storing the packets from both S and D before these packets are XORed and broadcasted by the relay. As such, the complexity of the Markov chain analysis increases exponentially with the number of relays (resp. two times the number of relays) in one-way (resp. two-way) BA networks.

A transmission rate optimization problem was formulated and solved in [10] in the case of infinite-size buffers. The strategy in [10] was based on the channel state information (CSI) and was built on the assumption that each one of the two buffers at R contains a large enough number of packets so that the maximum transmission rate is guaranteed. Rate maximization was also considered in [11] with large enough buffer sizes. In addition to the CSI, the states of the buffers were also taken into account in [11] where a heuristic algorithm was proposed to abridge the difficult exact problem formulation that follows from considering the special cases where the buffers are either full or empty. Large enough buffer sizes were also assumed in [12] that tackled rate maximization with a residual energy based relay selection approach for energy-constrained relays. [13] and [14], [15] considered throughput maximization in BA two-way networks with adaptive rate

The author is with the Department of Electrical and Computer Engineering of the Lebanese American University (LAU), PO box 36 Byblos 961, Lebanon. (e-mail: chadi.abourjeily@lau.edu.lb).

transmission and fixed rate transmission, respectively. In [14], [15], the optimal transmission mode is selected for maximizing the sum throughput in the delay unconstrained and delay constrained scenarios respectively. While the mode selection is SNR-based in the case of infinite buffer sizes in [14], the mode selection is based on both the quality of the links and the buffer state with finite size buffers in [15]. While the relaying schemes in [10]–[15] considered the transmission over an infinite number of time slots, a practical slot-by-slot two-way relaying scheme was proposed and studied in [16] based on a Markov chain analysis.

Two types of traffic were considered in [17]; namely, an up-link (UL) traffic and a down-link (DL) traffic. However, these two data traffics flow independently from each other since, unlike the considered two-way relaying scheme, these traffics are not XORed at the relay. For example, for the orthogonal scheme in [17], each time frame is divided into two slots; one for the UL and the other for the DL and, thus, the studied system is equivalent to two parallel one-way relaying systems. An amplify-and-forward (AF) two-way BA relaying scheme was proposed in [18]. This scheme enhances the reliability of the system through time-diversity where the same information packet is transmitted over several time slots, thus, incurring a sharp reduction in the effective throughput. Compared to [18], the proposed solution reduces the outage probability while transmitting each packet only once which positively impacts the network throughput. Moreover, storing the decoded binary packets in DF systems requires smaller buffer sizes compared to storing quantized values (over large number of levels) of the received samples for AF relaying. An adaptive rate two-way relaying scheme was proposed in [19] where the transmitted packet spans more than one fading block. This clearly differentiates [19] from our work that proposes a fixed rate block-by-block scheme. While the modulation and physical layer network coding were not addressed in [19], the proposed solution can be implemented with simpler transceivers since one coding and modulation scheme is needed for fixed rate transmission. Moreover, confining the packet transmission to a single fading block incurs smaller delays and lower complexities of the encoder and decoder. On the other hand, the implementation of [19] requires that a number of constraints on the time evolution of the channel states must be satisfied unlike the block-by-block scheme proposed in this work that does not impose any similar constraints. Finally, [19] adopts predefined scheduling where each time slot is divided into a multiple access phase that precedes the broadcast phase unlike our work that relaxes this restriction by allowing any node to transmit over consecutive time slots. Similar predefined scheduling was adopted in [20] and [21]. Two variants of two-way relaying were considered in these references differing by whether R transmits only XORed packets or can transmit a packet extracted from one of the buffers. The predefined scheduling clearly differentiates [20], [21] from our work. For example, for the Markov chain (MC) analysis considered in this paper, a state of the MC is completely defined by two parameters corresponding to the numbers of packets stored in the two buffers at R. On the other hand, a third parameter was added to the MC state in [20] forcing the MC to alternate between transmission from R and transmission from the users (eq. (2) in [20]). This alternation constrains the performance of the system and is not justified since R possesses storing capabilities and, hence, can transmit or receive over more than one consecutive slots. Finally, while our work considers relay buffers with small sizes, the queuing theoretic analysis in [21] assumes that the buffers are sufficiently large so that there are always spare spaces in the buffers. Moreover, while the relaying schemes in [20], [21] are heuristic, the proposed scheme is optimized to achieve the best OP and APD performance.

Two approaches can be adopted for designing BA relaying strategies. The first one is an ergodic approach based on considering an observation window comprising a number of time slots that tends to infinity [7], [10]–[15]. The second approach revolves around the design of practical slot-by-slot algorithms [3]–[6], [16], [20], [21]. While the first approach is more suitable for infinite and large buffer sizes, the second approach holds for any buffer size and, in particular, for small buffer sizes where the transient effects resulting from filling the buffer at the beginning of the transmission session and emptying it at the end of this session cannot be neglected.

In this work, we propose a novel slot-by-slot relaying strategy for BA DF two-way networks where the relay is equipped with buffers having practically-appealing finite sizes. The relaying protocol is completely controlled by two threshold parameters that are further optimized by considering three Quality-of-Service (QoS) indicators; namely, the OP, APD and diversity order. The capability of the proposed scheme in achieving optimal performance with finite size buffers clearly differentiates this scheme from (i): the existing heuristic algorithms in [11], [12], [15]–[21] that can be applied with finite size buffers and (ii): the optimal approaches in [10], [14] that hold only for infinite size buffers thus circumventing the need for implementing procedures that avoid the buffer overflow. A major stage in the performed optimization revolved around deriving simple closed-form expressions of the OP and APD for asymptotically large values of the SNR through a Markov chain analysis. These OP and APD expressions captured the dependence of the system performance on the threshold values and buffer sizes in an intuitive manner thus allowing for the formulation of simple design criteria. Motivated by the large values of the buffer sizes considered in the open literature on BA two-way relaying, a primary focus in this work is dedicated to the issue of the buffer size; in particular, determining the smallest buffers that can be deployed without jeopardizing the system performance. Denoting by L_1 and L_2 the sizes of the two buffers at the relay, [10]–[16], [21] assumed that $L_1 = L_2 = L$ with $L \to +\infty$ in [10], [13], [14], [21], $L = 500$ in [11], [12], $L = 10$ in [15] while values of L up to 40 were considered in [16]. In contrast to these large values, we prove that nothing can be gained from increasing (L_1, L_2) beyond $(3, 3)$ in the asymptotic regime with optimized relaying. Moreover, the buffer sizes of $(2, 3)$, $(3, 2)$ and $(2, 2)$ can also achieve a full diversity order with a reduced coding gain depending on the network topology in generalized $\kappa-\mu$ fading environments. Regarding the queuing delay, unlike the heuristic strategy in [16] where the asymptotic APD grows

linearly with L when L is big enough, the proposed scheme achieves the smaller asymptotic value of 3.5 for all values of L. In this regard, the appealing small values of the diversity-achieving buffer sizes and queuing delays follow as direct consequences of the adopted optimization methodology, thus, highlighting on the effectiveness of this approach.

II. System Model

A. Basic Parameters

Consider a three-node network, as depicted in Fig. 1, where no direct link is available between the nodes A and B that communicate with each other through a relay R. We assume that the nodes are equipped with a single antenna each. We also assume that all nodes are half-duplex (HD) and, hence, cannot transmit and receive simultaneously. The signals received at A, B and R are corrupted by an additive white Gaussian noise (AWGN) with zero mean and unit variance. We consider a flat block-fading channel model where the channel coefficients along the A-R and B-R links remain constant over a block fading duration and vary independently from one fading block to another. We denote by h_1 and h_2 the channel coefficients between A and R and between B and R, respectively. Finally, following from the channel reciprocity, the transmissions from R to A and from R to B experience the same fading coefficients h_1 and h_2, respectively.

While the adopted system model considers HD relaying in a way that is analogous to the majority of the existing one-way [3]–[9] and two-way [10]–[21] relaying systems, the research on full-duplex (FD) relaying is on the rise [2], [22]. While conventional HD relaying relies on transmitting and receiving in different time slots, FD operation supports concurrent transmission and reception thus improving the theoretical attainable spectral efficiency by a factor of two. However, in practice, HD relays may be preferred as they are easier to implement than FD relays that suffer from residual self-interference (SI) even after cancellation. In fact, the theoretical doubling of the throughput was not attained experimentally and heavy SI may even reduce the capacity of FD systems as compared to HD systems and may lead to oscillations within the transceivers rendering the communication system unstable [2]. Moreover, a network-level capacity analysis reveals that inter-link interference and spatial reuse substantially reduce the FD gain, rendering it well below the theoretical value of two in practical scenarios [22]. The proposed HD scheme can be extended to FD relaying by allowing for two additional transmission modes where A-and-R and B-and-R can transmit together. However, the achievable gains will be highly dependent on the levels of SI assumed. Moreover, as in [3]–[16], [18]–[21], we assume that the direct link between A and B does not exist because of shadowing and path-loss effects. If this link exists, the proposed scheme can be extended to a hybrid scheme that adaptively switches to the direct transmission mode if the direct link can support the target rate.

In this work, we adopt the generalized $\kappa-\mu$ fading model due to its wide applicability and generality [23]. The $\kappa-\mu$ distribution encompasses many well known fading models as special cases including the Rice, Nakagami-m, Rayleigh and one-sided Gaussian distributions. The communication link A-R is in outage if the corresponding channel capacity falls below the target rate r_0 (in bits per channel use (BPCU)). The outage probability along this link is denoted by p and can be determined from: $p=\Pr\left(\frac{1}{2}\log_2(1+\gamma|h_1|^2)<r_0\right)$ where γ stands for the average transmit signal-to-noise ratio (SNR) while the factor $1/2$ captures the fact that the communication between nodes A and B requires two time slots [3], [4]. Similarly, the link B-R is in outage with the following probability: $q=\Pr\left(\frac{1}{2}\log_2(1+\gamma|h_2|^2)<r_0\right)$. For the $\kappa-\mu$ fading model, the parameter κ describes the ratio between the powers of the dominant and scattered waves while the parameter μ denotes the number of multi-path clusters. Denoting by (κ_1,μ_1) and (κ_2,μ_2) the parameters of the $\kappa-\mu$ distribution associated with the links A-R and B-R, respectively, the outage probabilities can be determined from [23]:

$$p=1-Q_{\mu_1}\left(\sqrt{2\kappa_1\mu_1},\sqrt{2\mathfrak{r}\mu_1(1+\kappa_1)(\Omega_1\gamma)^{-1}}\right) \quad (1)$$

$$q=1-Q_{\mu_2}\left(\sqrt{2\kappa_2\mu_2},\sqrt{2\mathfrak{r}\mu_2(1+\kappa_2)(\Omega_2\gamma)^{-1}}\right), \quad (2)$$

where $Q_m(\cdot,\cdot)$ stands for the generalized Marcum Q-function while $\mathfrak{r}\triangleq 2^{2r_0}-1$. Finally, $\Omega_1=\mathrm{E}[|h_1|^2]$ and $\Omega_2=\mathrm{E}[|h_1|^2]$.

For asymptotically large values of the SNR, the outage probabilities in (1)-(2) tend to:

$$p\to\frac{e^{-\kappa_1\mu_1}}{\Gamma(\mu_1+1)}\left[\frac{\Omega_1\gamma}{\mathfrak{r}\mu_1(1+\kappa_1)}\right]^{-\mu_1};$$
$$q\to\frac{e^{-\kappa_2\mu_2}}{\Gamma(\mu_2+1)}\left[\frac{\Omega_2\gamma}{\mathfrak{r}\mu_2(1+\kappa_2)}\right]^{-\mu_2} \text{ as } \gamma\to\infty, \quad (3)$$

where $\Gamma(\cdot)$ stands for the gamma function. Equation (3) shows that the diversity orders[1] along the links A-R and B-R are equal to μ_1 and μ_2, respectively.

B. Packet Exchange and Buffering

The communication from a transmitting node is followed by short acknowledge/no-acknowledge (ACK/NACK) from the receiving node. The reception of a NACK or ACK message indicates whether the corresponding link is in outage or not, respectively. As depicted in Fig. 1, the relay is equipped with two buffers; one buffer, denoted by B_1, for storing the packets received from A and a second buffer, denoted by B_2, for storing the packets received from B. The sizes of these buffers are denoted by L_1 and L_2, respectively. Four modes arise in the network. (i): Node A is transmitting. The transmission of

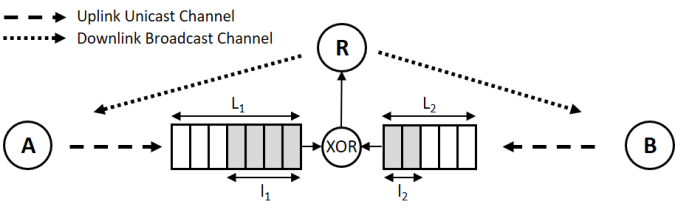

Fig. 1. Buffer-aided two-way decode-and-forward relaying system model.

[1]The diversity order is defined as the negative slope of the OP-versus-SNR curve when plotted on a log-log scale.

a packet from A to R necessitates that the link A-R is not in outage and that B_1 is not full. (ii): Node B is transmitting which can occur only if the link B-R is not in outage and B_2 is not full. (iii): The relay R is broadcasting a packet that is generated by XOR-ing a packet from A and a packet from B. At A, the packet from B can be reconstructed by XOR-ing the packet received from R with A's own packet. A similar reconstruction is implemented at B. As such, entering this mode necessitates the presence of at least one packet in B_1 and at least one packet in B_2. Moreover, both the R-A and R-B links must not suffer from outage so that the XOR-ed packet can reach both A and B. (iv): Finally, if none of the above transmission requirements are met, the network is in the idle mode and no node will be transmitting. Finally, in analogy with [10]–[16], we assume an infinite supply of data at A and B and we assume that these nodes are equipped with infinite-size buffers.

Regarding the order of reception of the packets, it's worth highlighting the following. (i): The buffers operate under the First-In-First-Out (FIFO) principle. (ii): There is no packet loss in the sense that the information packets are stored either in A's buffer, or in B's buffer or in R's buffers (until the channel conditions are favorable for these packets to be communicated without outage). (iii): R transmits only XORed packets to A and B. Therefore, the n-th transmission from R will involve the n-th packet from A (at the head of the buffer B_1) and the n-th packet from B (at the head of the buffer B_2). Therefore, no involved network coordination is needed for A and B to know which packets were XORed since the XORed packet transmitted from R in its n-th transmission epoch carries the n-th packet of A and the n-th packet of B. This simplicity of implementation clearly distinguishes the proposed scheme from the existing schemes [14]–[16], [20], [21] since, in these references, the XORed-message broadcasting is not imposed on R. As such, the packet overhead for these schemes must disadvantageously include A's packet number and B's packet number since the packets at the heads of the two buffer B_1 and B_2 might not have the same number unlike the scheme we propose.

C. Relaying Strategy

We denote by l_i the number of packets stored in B_i with $0 \leq l_i \leq L_i$ for $i = 1, 2$. The relaying scheme needs to incentivize R to receive when the numbers of stored packets are small and to transmit otherwise. The judgement on whether the numbers of packets are small or large is fixed by the two threshold levels $l_{\text{th}}^{(1)} \in \{0, \ldots, L_1\}$ and $l_{\text{th}}^{(2)} \in \{0, \ldots, L_2\}$. As such, considering the link A-R, the priority should be granted for A to transmit if $l_1 \leq l_{\text{th}}^{(1)}$ and for R to transmit if $l_1 > l_{\text{th}}^{(1)}$. The same holds for the link B-R where B transmits if $l_2 \leq l_{\text{th}}^{(2)}$ and R transmits if $l_2 > l_{\text{th}}^{(2)}$. Therefore, the relaying protocol selects the transmitting node according to the following priority. (i): If $l_1 > l_{\text{th}}^{(1)}$ and $l_2 > l_{\text{th}}^{(2)}$, priority is given to R that attempts to broadcast a XOR-ed packet to A and B. (ii): If $l_1 \leq l_{\text{th}}^{(1)}$ and $l_2 > l_{\text{th}}^{(2)}$, priority is given to A to transmit a packet to R. (iii): If $l_1 > l_{\text{th}}^{(1)}$ and $l_2 \leq l_{\text{th}}^{(2)}$, priority is given to B to transmit a packet to R. (iv): If $l_1 \leq l_{\text{th}}^{(1)}$ and $l_2 \leq l_{\text{th}}^{(2)}$, a selection must be made among A and B depending on the values of l_1 and l_2. In this case, priority should be given to filling the buffer having the smaller number of stored packets in order to avoid the saturation of the other buffer. In other words, priority should be given to A (resp. B) if $l_1 < l_2$ (resp. $l_1 > l_2$) and a random selection is made if $l_1 = l_2$.

Moreover, a node might lose its priority to transmit if the corresponding link/links on which it is attempting to transmit is/are in outage. This shift in the priority from one node to another consequences a more efficient use of the network time resources by avoiding the transmission over a channel that does not meet the target rate requirement. In other words, A loses its priority to transmit if the link A-R is in outage, B loses its priority to transmit if the link B-R is in outage and R loses its priority to transmit unless when both links R-A and R-B are not in outage. Consequently, the network enters in one of the four previously delineated modes as follows:

- If both the A-R and B-R links are in outage, the network is in the idle mode.
- If the A-R link is not in outage and the B-R link is in outage (with probability $(1-p)q$), node A is selected to transmit if the buffer B_1 is not full (so that the received packet can be accommodated). In this case, if B_1 is full, the network will be in the idle mode.
- If the A-R link is in outage and the B-R link is not in outage (with probability $p(1-q)$), node B is selected to transmit if $l_2 \neq L_2$ while no node will transmit otherwise.
- If both the A-R and B-R links are not in outage (with probability $(1-p)(1-q)$), the following selection strategy is implemented as rationalized before:

$$\begin{cases} l_1 > l_{\text{th}}^{(1)}\ ,\ l_2 > l_{\text{th}}^{(2)}, & R \ \text{Tx}; \\ l_1 \leq l_{\text{th}}^{(1)}\ ,\ l_2 > l_{\text{th}}^{(2)}, & A \ \text{Tx}; \\ l_1 > l_{\text{th}}^{(1)}\ ,\ l_2 \leq l_{\text{th}}^{(2)}, & B \ \text{Tx}; \\ l_1 \leq l_{\text{th}}^{(1)}\ ,\ l_2 \leq l_{\text{th}}^{(2)}, & \begin{cases} l_1 < l_2, & A \ \text{Tx}; \\ l_1 > l_2, & B \ \text{Tx}; \\ l_1 = l_2, & A \text{ or B Tx}. \end{cases} \end{cases}, \tag{4}$$

Finally, from (4), the threshold levels must satisfy the following relation:

$$l_{\text{th}}^{(1)} \neq L_1 \ \ ; \ \ l_{\text{th}}^{(2)} \neq L_2, \tag{5}$$

since, otherwise, the relations $l_1 > l_{\text{th}}^{(1)}$ and $l_2 > l_{\text{th}}^{(2)}$ cannot be satisfied and R can never transmit.

The exchange of signaling messages is orchestrated by R. Based on the numbers of stored packets at R (l_1 and l_2) and on the availability of the A-R and R-B links (acquired through the exchange of ACK/NACK signals with R), R makes a decision on which node must transmit at each time slot. R then shares this decision with A and B by broadcasting a short signaling message that precedes the information message in each time slot. Since the network comprises three nodes, a 2-bit signaling message is sufficient for informing the nodes on the single node that was selected to transmit. This signaling overhead is judged to be very small and, hence, it does not affect the effective throughput of the network. This signaling overhead is also smaller than that of [14]–[16], [20], [21]. In fact, for

these references, the signaling message broadcasted from R must include an additional bit since A and B can transmit together, R can transmit to A alone and R can transmit to B alone (for example, refer to Table I in [14], [15]).

III. Performance Analysis

In this section, we carry out a Markov chain analysis to evaluate the steady-state distribution, OP and APD. A state of the Markov chain is represented by the numbers of packets present in the two buffers (l_1, l_2) resulting in a total of $N_s \triangleq (L_1+1)(L_2+1)$ possible states.

A. Transition Probabilities

We denote by $t_{(l_1,l_2),(l_1',l_2')}$ the transition probability of moving from the state (l_1, l_2) to the state (l_1', l_2'). The transition probabilities satisfy the following relation:

$$\sum_{l_1'=0}^{L_1}\sum_{l_2'=0}^{L_2} t_{(l_1,l_2),(l_1',l_2')} = 1 \quad \forall \ \ (l_1,l_2) \in \{0,\ldots,L_1\}\times\{0,\ldots,L_2\}. \quad (6)$$

In what follows, $t_{(l_1,l_2),(l_1',l_2')} = 0$ if the new state $(l_1', l_2') \notin \{0,\ldots,L_1\}\times\{0,\ldots,L_2\}$. The transition probabilities will be determined in the four following cases following from (4).

1) Case I: $l_1 > l_{\text{th}}^{(1)}$ and $l_2 > l_{\text{th}}^{(2)}$ where the priority is given to the transmission from R. In this case, if both the R-A and R-B links are not in outage, then R successfully manages to communicate the XOR-ed packet to both A and B. Consequently, a packet is freed from B_1 and another packet is freed from B_2 for the sake of generating the XOR-ed packet. This results in:

$$t_{(l_1,l_2),(l_1-1,l_2-1)} = (1-p)(1-q). \quad (7)$$

When the link A-R is not in outage while the link B-R is in outage, it is only meaningful for A to transmit. In this case, B_1 can accommodate for the incoming packet only if this buffer is not full resulting in:

$$t_{(l_1,l_2),(l_1+1,l_2)} = (1-p)q\delta_{l_1\neq L_1}, \quad (8)$$

where $\delta_S = 1$ if the statement S is true and $\delta_S = 0$ otherwise.

Similarly, when the link A-R is in outage while the link B-R is not in outage, B is selected to transmit and the number of packets in B_2 will increase by one if it was not initially full:

$$t_{(l_1,l_2),(l_1,l_2+1)} = p(1-q)\delta_{l_2\neq L_2}. \quad (9)$$

Finally, the network remains idle if (i): both hops are in outage, (ii): A is selected for transmission but B_1 is full or (iii): B is selected for transmission but B_2 is full:

$$t_{(l_1,l_2),(l_1,l_2)} = pq + (1-p)q\delta_{l_1=L_1} + p(1-q)\delta_{l_2=L_2}. \quad (10)$$

2) Case II: $l_1 \leq l_{\text{th}}^{(1)}$ and $l_2 > l_{\text{th}}^{(2)}$. Since the priority is given to A, then:

$$t_{(l_1,l_2),(l_1+1,l_2)} = 1-p, \quad (11)$$

regardless of the state of link B-R. Equation (11) implies that a packet can be readily delivered from A to R if the link A-R is not in outage since the relation $l_1 \leq l_{\text{th}}^{(1)}$ and $l_{\text{th}}^{(1)} \neq L_1$ (from (5)) implies that $l_1 \neq L_1$ and buffer B_1 is not full.

On the other hand, if the link A-R is in outage, priority shifts to B. In this case, the number of packets stored in B_2 will either increase by one if the link B-R is not in outage and this buffer is not full or it will remain the same otherwise:

$$t_{(l_1,l_2),(l_1,l_2+1)} = p(1-q)\delta_{l_2\neq L_2} \quad (12)$$

$$t_{(l_1,l_2),(l_1,l_2)} = pq + p(1-q)\delta_{l_2=L_2}. \quad (13)$$

3) Case III: $l_1 > l_{\text{th}}^{(1)}$ and $l_2 \leq l_{\text{th}}^{(2)}$ where the transmission priority is given to B. Interchanging the roles of nodes A and B in (11), (12) and (13) results in:

$$t_{(l_1,l_2),(l_1,l_2+1)} = 1-q, \quad (14)$$

$$t_{(l_1,l_2),(l_1+1,l_2)} = (1-p)q\delta_{l_1\neq L_1} \quad (15)$$

$$t_{(l_1,l_2),(l_1,l_2)} = pq + (1-p)q\delta_{l_1=L_1}. \quad (16)$$

4) Case IV: $l_1 \leq l_{\text{th}}^{(1)}$ and $l_2 \leq l_{\text{th}}^{(2)}$ where a node among A and B is selected to transmit. The numbers of stored packets will remain the same if both A-R and B-R links are in outage:

$$t_{(l_1,l_2),(l_1,l_2)} = pq. \quad (17)$$

On the other hand:

$$t_{(l_1,l_2),(l_1+1,l_2)} = (1-p)\left[q + (1-q)\left(\delta_{l_1<l_2} + \frac{1}{2}\delta_{l_1=l_2}\right)\right], \quad (18)$$

where l_1 can increase by one only if the link A-R is not in outage. In this case, the selection of A (rather than B) to transmit is triggered because of one of the following reasons. (i): The link B-R is in outage. (ii): The link B-R is not in outage but B_1 contains a smaller number of stored packets compared to B_2. (iii): The link B-R is not in outage and $l_1 = l_2$ entailing a random selection among A and B where each one of these nodes can be selected with probability $1/2$.

Similar to (18):

$$t_{(l_1,l_2),(l_1,l_2+1)} = (1-q)\left[p + (1-p)\left(\delta_{l_1>l_2} + \frac{1}{2}\delta_{l_1=l_2}\right)\right]. \quad (19)$$

B. Steady-State Probability Distribution

The transition probabilities will be stacked to form the $N_s \times N_s$ state transition matrix $\mathbf{T}$:

$$\mathbf{T}_{\psi(l_1',l_2'),\psi(l_1,l_2)} = t_{(l_1,l_2),(l_1',l_2')}, \quad (20)$$

where the function $\psi(\cdot)$ is used to number the states and it defines a one-to-one relation between the set of all possible states $\{0,\ldots,L_1\}\times\{0,\ldots,L_2\}$ and the set of integers $\{1,\ldots,N_s\}$:

$$\psi(l_1,l_2) = l_1(L_2+1) + l_2 + 1. \quad (21)$$

The matrix $\mathbf{T}$ is used to evaluate the steady-state probability distribution vector $\mathbf{\Pi}$ [3]–[5]:

$$\mathbf{\Pi} = (\mathbf{T} - \mathbf{I} + \mathbf{V})^{-1} \mathbf{v}, \tag{22}$$

where $\mathbf{I}$ and $\mathbf{V}$ are $N_s \times N_s$ matrices denoting the identity matrix and all-one matrix, respectively. Vector $\mathbf{v}$ is the N_s-dimensional vector whose elements are all equal to 1.

At steady-state, the probability of having l_1 packets stored in B_1 and l_2 packets stored in B_2 will be denoted by π_{l_1,l_2} and can be determined from:

$$\pi_{l_1,l_2} = \mathbf{\Pi}_n \quad | \quad \psi(l_1,l_2) = n, \tag{23}$$

where $\mathbf{\Pi}_n$ stands for the n-th element of the vector $\mathbf{\Pi}$ in (22). Following from the joint distribution in (23), the marginal distributions can be determined from:

$$\pi_{l_1}^{(1)} = \sum_{l_2=0}^{L_2} \pi_{l_1,l_2} \quad ; \quad \pi_{l_2}^{(2)} = \sum_{l_1=0}^{L_1} \pi_{l_1,l_2}, \tag{24}$$

where $\pi_l^{(k)}$ stands for the probability of having l packets stored in B_k at steady-state for $l = 0, \ldots, L_k$ and $k = 1, 2$.

C. Outage Probability

The network will be in outage if no packets can be communicated along the constituent links resulting in the four following cases. (i): If both the A-R and B-R links are in outage, then no packets can be transferred along any of these links and the system will suffer from outage. (ii): If the link A-R is not in outage and the link B-R is in outage, then A is allowed to transmit in this case. Since the A-R link is not in outage, a packet can always be delivered to R unless if B_1 is full. (iii): Similar to the previous case, if the link A-R is in outage and the link B-R is not in outage, the system will suffer from outage if B_2 is full since no packet can be transmitted from B to R in this case. (iv): If the A-R and B-R links are not in outage, the system will not be in outage. In fact, if $l_1 > l_{\text{th}}^{(1)}$ and $l_2 > l_{\text{th}}^{(2)}$, a XOR-ed packet can be transmitted from R to both A and B. If $l_1 \leq l_{\text{th}}^{(1)}$ and $l_2 > l_{\text{th}}^{(2)}$ (resp. $l_1 > l_{\text{th}}^{(1)}$ and $l_2 \leq l_{\text{th}}^{(2)}$), then A (resp. B) can successfully transmit a packet to R and this packet can be stored in B_1 (resp. B_2) following from (5). Finally, if $l_1 \leq l_{\text{th}}^{(1)}$ and $l_2 \leq l_{\text{th}}^{(2)}$, a packet can be delivered from either A or B to R. Following from the above four considered cases, the system outage probability is given by:

$$P_{\text{out}} = pq + (1-p)q\pi_{L_1}^{(1)} + p(1-q)\pi_{L_2}^{(2)}, \tag{25}$$

where $\pi_{L_1}^{(1)}$ and $\pi_{L_2}^{(2)}$ stand for the probabilities of having B_1 and B_2 full, respectively.

D. Average Packet Delay

Because of the queuing at the buffers of A and R, the packets generated from A will arrive at B with a queuing delay denoted by D_A. Similarly, we denote by D_B the average delay for the packets generated at B to reach A where this delay follows form the buffering at B_2 and at B's buffer. Consequently, the average packet delay (APD) of the two-way relaying network is given by:

$$D = \frac{D_A + D_B}{2}. \tag{26}$$

We denote by η_A the average output throughput from node A which is equivalent to the input throughput at B_1 since the relaying scheme in (4) circumvents the packet loss by stopping the reception when the buffer is full. Evidently, a packet can depart from A's buffer only if the link A-R is not in outage. As such, the following two cases arise depending on whether the link B-R is in outage or not. (i): If the link B-R is in outage, then A is selected to transmit and a packet can be delivered to R only if B_1 is not full with probability $1 - \pi_{L_1}^{(1)}$. (ii): If the link B-R is not in outage, then either A, B or R can transmit depending on the values of l_1 and l_2 according to (4). If $l_1 > l_{\text{th}}^{(1)}$ and $l_2 > l_{\text{th}}^{(2)}$, R will transmit and no packet can depart from A's buffer. Similarly, if $l_1 > l_{\text{th}}^{(1)}$ and $l_2 \leq l_{\text{th}}^{(2)}$, B is selected to transmit and no packet can exit A's buffer. If $l_1 \leq l_{\text{th}}^{(1)}$ and $l_2 > l_{\text{th}}^{(2)}$, A is selected to transmit thus contributing to increasing the output throughput from A. Finally, if $l_1 \leq l_{\text{th}}^{(1)}$ and $l_2 \leq l_{\text{th}}^{(2)}$, then according to (4), A can always transmit if $l_1 < l_2$ while it transmits half of the time if $l_1 = l_2$. Therefore, η_A can be determined from:

$$\eta_A = (1-p)\left[q\left(1 - \pi_{L_1}^{(1)}\right) + (1-q)\sum_{l_1=0}^{L_1}\sum_{l_2=0}^{L_2}\pi_{l_1,l_2}\times \left[\delta_{l_1 \leq l_{\text{th}}^{(1)}}\delta_{l_2 > l_{\text{th}}^{(2)}} + \delta_{l_1 \leq l_{\text{th}}^{(1)}}\delta_{l_2 \leq l_{\text{th}}^{(2)}}\left(\delta_{l_1 < l_2} + \frac{1}{2}\delta_{l_1 = l_2}\right)\right]\right]. \tag{27}$$

Similarly, the average output throughput from node B can be determined from:

$$\eta_B = (1-q)\left[p\left(1 - \pi_{L_2}^{(2)}\right) + (1-p)\sum_{l_1=0}^{L_1}\sum_{l_2=0}^{L_2}\pi_{l_1,l_2}\times \left[\delta_{l_1 > l_{\text{th}}^{(1)}}\delta_{l_2 \leq l_{\text{th}}^{(2)}} + \delta_{l_1 \leq l_{\text{th}}^{(1)}}\delta_{l_2 \leq l_{\text{th}}^{(2)}}\left(\delta_{l_1 > l_2} + \frac{1}{2}\delta_{l_1 = l_2}\right)\right]\right]. \tag{28}$$

The delay D_A can be determined from [24], [25]:

$$D_A = \frac{\bar{L}^{(1)}}{\eta_A} + \frac{1}{\eta_A} - 1, \tag{29}$$

where $\bar{L}^{(k)} = \sum_{l=0}^{L_k} l\pi_l^{(k)}$ is the average queue length of buffer B_k for $k = 1, 2$. The term $\frac{\bar{L}^{(1)}}{\eta_A}$ corresponds to the average delay at B_1 and it follows from applying Little's law [24]. The term $\frac{1}{\eta_A} - 1$ corresponds to the average delay at the infinite-size buffer at A [25]. In fact, the number of trials to successfully transmit a packet from A follows the geometric distribution with parameter η_A resulting in an average number of trials of $\frac{1}{\eta_A}$. The subtraction of 1 from this average follows since a successful transmission attempt at trail i incurs a delay of $i - 1$ (for $i \geq 1$).

Similar to (29), D_B can be determined from:

$$D_B = \frac{\bar{L}^{(2)}}{\eta_B} + \frac{1}{\eta_B} - 1. \tag{30}$$

$$\mathbf{M}_1^{(1)}=\begin{bmatrix} \frac{1-p-2q}{3} & \frac{2p}{3} & 0 \\ \frac{1-2p}{3} & \frac{1-q}{3} & \frac{p}{3} \\ \frac{q}{3} & \frac{2q}{3} & 0 \end{bmatrix} \; ; \; \mathbf{M}_2^{(1)}=\begin{bmatrix} \frac{3-5p-3q}{9} & \frac{3-2p-6q}{9} & \frac{p}{3} \\ \frac{2q}{3} & \frac{3-2p}{9} & \frac{2p}{3} \\ 0 & \frac{q}{3} & 0 \end{bmatrix} \; ; \; \mathbf{M}_3^{(1)}=\begin{bmatrix} \frac{6-8p-9q}{18} & \frac{6+10p-15q}{36} & \frac{p}{6} \\ \frac{6-14p+15q}{36} & \frac{6-2p-3q}{18} & \frac{p}{2} \\ \frac{q}{6} & \frac{q}{2} & 0 \end{bmatrix}. \quad (36)$$

IV. Optimizing the Relaying Parameters

A. Order-0 Asymptotic Steady-State Distribution

For asymptotically large values of the SNR, $p \ll 1$ and $q \ll 1$. The order-0 asymptotic analysis is based on setting $p \to 0$ and $q \to 0$ in all the transition probabilities provided in Section III-A. In other words, the transition probabilities will assume one of the two values of 0 or 1 while all non-zero powers of the probabilities p and q will be set to zero. Consequently, the steady-state probabilities in (22) will tend to constants. This type of analysis is sufficient for drawing preliminary conclusions regarding the effect of the values of $l_{\text{th}}^{(1)}$ and $l_{\text{th}}^{(2)}$ on the outage probability as will be highlighted in Section IV-C. The order-0 asymptotic analysis is also appropriate for deriving exact values of the asymptotic APD as will be highlighted in Section IV-D.

We denote by $\mathbf{\Pi}^{(0)}$ the 2×2 matrix given by:

$$\mathbf{\Pi}^{(0)} = \begin{bmatrix} \pi_{l_{\text{th}}^{(1)},l_{\text{th}}^{(2)}} & \pi_{l_{\text{th}}^{(1)},l_{\text{th}}^{(2)}+1} \\ \pi_{l_{\text{th}}^{(1)}+1,l_{\text{th}}^{(2)}} & \pi_{l_{\text{th}}^{(1)}+1,l_{\text{th}}^{(2)}+1} \end{bmatrix}, \quad (31)$$

where, from (5), $l_{\text{th}}^{(1)} \leq L_1 - 1$ and $l_{\text{th}}^{(2)} \leq L_2 - 1$.

Proposition *1:* For $p \to 0$ and $q \to 0$, all the steady-state probabilities not included in $\mathbf{\Pi}^{(0)}$ will tend to zero while:

$$\mathbf{\Pi}^{(0)} \to \begin{cases} \mathbf{M}_1^{(0)}, & l_{\text{th}}^{(1)} < l_{\text{th}}^{(2)}; \\ \mathbf{M}_2^{(0)}, & l_{\text{th}}^{(1)} > l_{\text{th}}^{(2)}; \\ \mathbf{M}_3^{(0)}, & l_{\text{th}}^{(1)} = l_{\text{th}}^{(2)}. \end{cases}, \quad (32)$$

where:

$$\mathbf{M}_1^{(0)}=\begin{bmatrix} \frac{1}{3} & 0 \\ \frac{1}{3} & \frac{1}{3} \end{bmatrix} \; ; \; \mathbf{M}_2^{(0)}=\begin{bmatrix} \frac{1}{3} & \frac{1}{3} \\ 0 & \frac{1}{3} \end{bmatrix} \; ; \; \mathbf{M}_3^{(0)}=\begin{bmatrix} \frac{1}{3} & \frac{1}{6} \\ \frac{1}{6} & \frac{1}{3} \end{bmatrix}. \quad (33)$$

Proof: The proof is provided in Appendix A. ∎

B. Order-1 Asymptotic Steady-State Distribution

The order-0 asymptotic analysis provided in the previous subsection does not yield highly accurate asymptotic OP results when $l_{\text{th}}^{(1)} \leq L_1 - 2$ or $l_{\text{th}}^{(2)} \leq L_2 - 2$. Therefore, in this subsection, we resort to an order-1 asymptotic analysis by keeping only the constants, the term p and the term q while ignoring all higher powers of the probabilities p and q. In other words, we neglect all terms of the form $p^i q^j$ for $i+j > 1$ in the transition probabilities in (7)-(19). Consequently, the steady-state probabilities in (22) will be approximated by expressions of the form $a_0 + a_1 p + a_2 q$ (where a_0, a_1 and a_2 are constants) for $p \ll 1$ and $q \ll 1$.

For $l_{\text{th}}^{(1)} \leq L_1 - 2$ and $l_{\text{th}}^{(2)} \leq L_2 - 2$, we denote by $\mathbf{\Pi}^{(1)}$ the 3×3 matrix given by:

$$\mathbf{\Pi}^{(1)} = \begin{bmatrix} \pi_{l_{\text{th}}^{(1)},l_{\text{th}}^{(2)}} & \pi_{l_{\text{th}}^{(1)},l_{\text{th}}^{(2)}+1} & \pi_{l_{\text{th}}^{(1)},l_{\text{th}}^{(2)}+2} \\ \pi_{l_{\text{th}}^{(1)}+1,l_{\text{th}}^{(2)}} & \pi_{l_{\text{th}}^{(1)}+1,l_{\text{th}}^{(2)}+1} & \pi_{l_{\text{th}}^{(1)}+1,l_{\text{th}}^{(2)}+2} \\ \pi_{l_{\text{th}}^{(1)}+2,l_{\text{th}}^{(2)}} & \pi_{l_{\text{th}}^{(1)}+2,l_{\text{th}}^{(2)}+1} & \pi_{l_{\text{th}}^{(1)}+2,l_{\text{th}}^{(2)}+2} \end{bmatrix}. \quad (34)$$

Proposition *2:* For $p \ll 1$ and $q \ll 1$, all the steady-state probabilities not included in $\mathbf{\Pi}^{(1)}$ will tend to zero while:

$$\mathbf{\Pi}^{(1)} \to \begin{cases} \mathbf{M}_1^{(1)}, & l_{\text{th}}^{(1)} < l_{\text{th}}^{(2)}; \\ \mathbf{M}_2^{(1)}, & l_{\text{th}}^{(1)} > l_{\text{th}}^{(2)}; \\ \mathbf{M}_3^{(1)}, & l_{\text{th}}^{(1)} = l_{\text{th}}^{(2)}. \end{cases}, \quad (35)$$

where the matrices $\mathbf{M}_1^{(1)}$, $\mathbf{M}_2^{(1)}$ and $\mathbf{M}_3^{(1)}$ are provided in (36) on the top of the page.

Proof: The proof is provided in Appendix B. ∎

For $p \to 0$ and $q \to 0$, the first two rows and first two columns of the matrix $\mathbf{M}_i^{(1)}$ in (36) will tend to the matrix $\mathbf{M}_i^{(0)}$ in (33) for $i = 1, 2, 3$.

While the order-0 (resp. order-1) asymptotic analysis involves 4 (resp. 9) states and holds for $l_{\text{th}}^{(i)} \leq L_i - 1$ (resp. $l_{\text{th}}^{(i)} \leq L_i - 2$) for $i = 1, 2$, it can be easily proven that the order-n asymptotic analysis will involve $(n+2)^2$ states and will hold for $l_{\text{th}}^{(i)} \leq L_i - n - 1$ (for $i = 1, 2$) for any $0 \leq n \leq \min(L_1, L_2) - 1$. As such, determining the steady-state distribution will incur solving $(n+1)^2$ equations in $(n+1)^2$ unknowns. For $n \geq 2$, not only such solution might be hard to obtain in closed form, but also the order-n asymptotic analysis in this case will not provide any further insights since probabilities of the form $p^i q^j$ for $i + j > 1$ are several orders of magnitude smaller than the probabilities p and q for large SNRs. Therefore, an order-n asymptotic analysis with $n \geq 2$ will not affect the findings reached in this work pertaining to the diversity order as well as minimizing the asymptotic OP and asymptotic APD.

C. Asymptotic OP Analysis and Diversity Order

Full buffers will contribute to the system outage according to the relation provided in (25). The probability $\pi_{L_1}^{(1)}$ assumes the following asymptotic values:

$$\pi_{L_1}^{(1)} = \begin{cases} \beta_1, & l_{\text{th}}^{(1)} = L_1 - 1; \\ \beta_2 q, & l_{\text{th}}^{(1)} = L_1 - 2; \\ 0, & l_{\text{th}}^{(1)} < L_1 - 2. \end{cases}, \quad (37)$$

where the constants β_1 and β_2 are provided in Table I. The first and second probabilities in (37) are obtained by adding up the elements of the last rows of the matrices $\mathbf{M}_i^{(0)}$ and $\mathbf{M}_i^{(1)}$ in (33) and (36), respectively. The value of zero in (37) follows from (34) and proposition 2 that suggest that the probability $\pi_{l_1}^{(1)}$ will tend to zero for all $l_1 > l_{\text{th}}^{(1)} + 2$.

Similarly, inspecting the last columns of the matrices $\mathbf{M}_i^{(0)}$ and $\mathbf{M}_i^{(1)}$ in (33) and (36), in addition to (34) and proposition 2, the asymptotic values of the probability $\pi_{L_2}^{(2)}$ can be obtained from:

$$\pi_{L_2}^{(2)} = \begin{cases} \beta_3, & l_{\text{th}}^{(2)} = L_2 - 1; \\ \beta_4 p, & l_{\text{th}}^{(2)} = L_2 - 2; \\ 0, & l_{\text{th}}^{(2)} < L_2 - 2. \end{cases}, \quad (38)$$

TABLE I
VALUES OF THE PROBABILITIES β_1, β_2, β_3 AND β_4 IN (37) AND (38)

	$l_{\text{th}}^{(1)} < l_{\text{th}}^{(2)}$	$l_{\text{th}}^{(1)} > l_{\text{th}}^{(2)}$	$l_{\text{th}}^{(1)} = l_{\text{th}}^{(2)}$
β_1	$2/3$	$1/3$	$1/2$
β_2	1	$1/3$	$2/3$
β_3	$1/3$	$2/3$	$1/2$
β_4	$1/3$	1	$2/3$

where the constants β_3 and β_4 are provided in Table I.

Following from (25), (37) and (38), the asymptotic value of the OP depends on the relative values that the parameters $l_{\text{th}}^{(1)}$ and $l_{\text{th}}^{(2)}$ assume with respect to L_1 and L_2, respectively, according to the relations summarized in Table III. Following from the results in Table III, the following design criterion can be reached.

Criterion *1:* The asymptotic OP can be minimized by selecting any threshold levels $(l_{\text{th}}^{(1)}, l_{\text{th}}^{(2)})$ satisfying $l_{\text{th}}^{(1)} < L_1 - 2$ and $l_{\text{th}}^{(2)} < L_2 - 2$. The minimum achievable asymptotic OP in this case is equal to pq.

From (3), it can be observed that the probability pq scales asymptotically as $\gamma^{-\mu_1-\mu_2}$ resulting in the diversity order of $\mu_1 + \mu_2$. This diversity order of $\mu_1 + \mu_2$ will be referred to as the maximum achievable diversity order in what follows. On the other hand, a buffer-free system is not in outage only when both hops are not in outage resulting in an OP of $1 - (1-p)(1-q) \approx p + q - pq$. In this case, the performance is dominated by the worst of the two hops and the corresponding diversity order is equal to $\min\{\mu_1, \mu_2\}$. It is worth highlighting that the Rayleigh distribution follows as a special case of the generalized $\kappa - \mu$ distribution by setting $\mu = 1$. As such, while the maximum achievable diversity order over Rayleigh fading channels is equal to $\mu_1 + \mu_2 = 2$ (since $\mu_1 = \mu_2 = 1$), the maximum diversity order $\mu_1 + \mu_2$ can exceed two for the generalized $\kappa - \mu$ fading since, in general, $\mu_1 \geq 1$ and $\mu_2 \geq 1$.

Following from the asymptotic OP values provided in Table III, the corresponding diversity orders can be determined as summarized in Table II. In carrying out the diversity order analysis, the probabilities pq, p^2 and q^2 are neglected compared to the probabilities p and q. Moveover, if the probabilities r and s scale asymptotically as $\gamma^{-\mu_r}$ and $\gamma^{-\mu_s}$, respectively, then the term $r + s$ will scale asymptotically as $\gamma^{-\min\{\mu_r, \mu_s\}}$.

From Table II, it can be observed that the maximum diversity order of $\mu_1 + \mu_2$ can never be achieved if either $l_{\text{th}}^{(1)} = L_1 - 1$ or $l_{\text{th}}^{(2)} = L_2 - 1$. In a more general manner, the following diversity order-maximizing design criterion holds.

Criterion *2:* The maximum diversity order of $\mu_1 + \mu_2$ can be achieved by selecting the threshold values $l_{\text{th}}^{(1)}$ and $l_{\text{th}}^{(2)}$ as follows:

- For $\mu_1 < \mu_2$: $l_{\text{th}}^{(1)} \leq L_1 - 2$ and $l_{\text{th}}^{(2)} < L_2 - 2$.
- For $\mu_1 > \mu_2$: $l_{\text{th}}^{(1)} < L_1 - 2$ and $l_{\text{th}}^{(2)} \leq L_2 - 2$.
- For $\mu_1 = \mu_2$: $l_{\text{th}}^{(1)} \leq L_1 - 2$ and $l_{\text{th}}^{(2)} \leq L_2 - 2$.

Considering the choices that maximize the diversity order according to criterion 2, the coding gain is maximized by selecting $l_{\text{th}}^{(1)} < L_1 - 2$ and $l_{\text{th}}^{(2)} < L_2 - 2$ following from criterion 1. Compared to this selection, fixing $l_{\text{th}}^{(1)} = L_1 - 2$ and/or $l_{\text{th}}^{(2)} = L_2 - 2$ results in the asymptotic losses (in dB) provided in (39) at the bottom of the page. The constants β_2 and β_4 are given in Table I while $a_i = \frac{e^{-\kappa_i \mu_i}}{\Gamma(\mu_i+1)}$ and $b_i = \frac{\Omega_i}{\mathfrak{r}\mu_i(1+\kappa_i)}$ for $i = 1, 2$ following from (3).

D. Asymptotic APD Analysis

Following from (31) and proposition 1, equation (27) can be written as follows for asymptotic values of the SNR:

$$\eta_A = (1-p)\left[q\left(1 - \pi_{L_1}^{(1)}\right) + (1-q)S_A\right], \tag{40}$$

where the summation S_A is given by:

$$S_A = \pi_{l_{\text{th}}^{(1)}, l_{\text{th}}^{(2)}+1} + \pi_{l_{\text{th}}^{(1)}, l_{\text{th}}^{(2)}}\left[\delta_{l_{\text{th}}^{(1)} < l_{\text{th}}^{(2)}} + \frac{1}{2}\delta_{l_{\text{th}}^{(1)} = l_{\text{th}}^{(2)}}\right]. \tag{41}$$

Following from (33), the following three cases arise. (i): $l_{\text{th}}^{(1)} < l_{\text{th}}^{(2)}$ implying that $S_A = 0 + \frac{1}{3} \times 1 = \frac{1}{3}$. (ii): $l_{\text{th}}^{(1)} > l_{\text{th}}^{(2)}$ implying that $S_A = \frac{1}{3} + \frac{1}{3} \times 0 = \frac{1}{3}$. (iii): $l_{\text{th}}^{(1)} = l_{\text{th}}^{(2)}$ resulting in $S_A = \frac{1}{6} + \frac{1}{3} \times \frac{1}{2} = \frac{1}{3}$. Therefore, $S_A = \frac{1}{3}$ in all cases and (40) simplifies to:

$$\eta_A = (1-p)\left[q\left(1 - \pi_{L_1}^{(1)}\right) + \frac{1-q}{3}\right] \approx \frac{(1-p)(1-q)}{3}, \tag{42}$$

since, from (37), the probability $\pi_{L_1}^{(1)}$ is either zero, or constant or proportional to q and, hence, the term $q\left(1 - \pi_{L_1}^{(1)}\right)$ can be neglected asymptotically.

Similar calculations show that the asymptotic expression of (28) is given by:

$$\eta_B = (1-q)\left[p\left(1 - \pi_{L_2}^{(2)}\right) + \frac{1-p}{3}\right] \approx \frac{(1-p)(1-q)}{3}. \tag{43}$$

$$\begin{cases} \frac{10}{\mu_1+\mu_2}\log_{10}\left(1 + \beta_2 \frac{a_2 b_1^{\mu_1}}{a_1 b_2^{\mu_2}}\right), & l_{\text{th}}^{(1)} = L_1 - 2 \text{ (if } \mu_1 \leq \mu_2); \\ \frac{10}{\mu_1+\mu_2}\log_{10}\left(1 + \beta_4 \frac{a_1 b_2^{\mu_2}}{a_2 b_1^{\mu_1}}\right), & l_{\text{th}}^{(2)} = L_2 - 2 \text{ (if } \mu_1 \geq \mu_2); \\ \frac{10}{\mu_1+\mu_2}\log_{10}\left(1 + \beta_2 \frac{a_2 b_1^{\mu_1}}{a_1 b_2^{\mu_2}} + \beta_4 \frac{a_1 b_2^{\mu_2}}{a_2 b_1^{\mu_1}}\right), & l_{\text{th}}^{(1)} = L_1 - 2 \ \& \ l_{\text{th}}^{(2)} = L_2 - 2 \text{ (if } \mu_1 = \mu_2). \end{cases}, \tag{39}$$

TABLE II
ACHIEVABLE DIVERSITY ORDERS

	$l_{\text{th}}^{(2)} < L_2 - 2$	$l_{\text{th}}^{(2)} = L_2 - 2$	$l_{\text{th}}^{(2)} = L_2 - 1$
$l_{\text{th}}^{(1)} < L_1 - 2$	$\mu_1 + \mu_2$	$\mu_1 + \min\{\mu_1, \mu_2\}$	μ_1
$l_{\text{th}}^{(1)} = L_1 - 2$	$\mu_2 + \min\{\mu_1, \mu_2\}$	$2\min\{\mu_1, \mu_2\}$	μ_1
$l_{\text{th}}^{(1)} = L_1 - 1$	μ_2	μ_2	$\min\{\mu_1, \mu_2\}$

Similarly, the asymptotic values of the average queue lengths can be determined from (33) as follows:

$$(\bar{L}^{(1)}, \bar{L}^{(2)}) = \begin{cases} \left(l_{\text{th}}^{(1)} + \frac{2}{3}, l_{\text{th}}^{(2)} + \frac{1}{3}\right), & l_{\text{th}}^{(1)} < l_{\text{th}}^{(2)}; \\ \left(l_{\text{th}}^{(1)} + \frac{1}{3}, l_{\text{th}}^{(2)} + \frac{2}{3}\right), & l_{\text{th}}^{(1)} > l_{\text{th}}^{(2)}; \\ \left(l_{\text{th}}^{(1)} + \frac{1}{2}, l_{\text{th}}^{(2)} + \frac{1}{2}\right), & l_{\text{th}}^{(1)} = l_{\text{th}}^{(2)}. \end{cases} \quad (44)$$

Replacing (42) and (43) in (29) and (30), respectively, results in $D_A = 3\bar{L}^{(1)} + 2$ and $D_B = 3\bar{L}^{(2)} + 2$ where the term $(1-p)(1-q)$ in (42) and (43) was approximated by 1 for $p \ll 1$ and $q \ll 1$. Therefore, from (26), $D = \frac{3}{2}(\bar{L}^{(1)} + \bar{L}^{(2)}) + 2$. From (44), it can be observed that the summation $\bar{L}^{(1)} + \bar{L}^{(2)}$ assumes the same value in all cases. Consequently, the asymptotic APD can be determined from the following expression:

$$D = \frac{3}{2}\left(l_{\text{th}}^{(1)} + l_{\text{th}}^{(2)}\right) + \frac{7}{2} \quad \forall \quad l_{\text{th}}^{(1)} \leq L_1 - 1 \;\&\; l_{\text{th}}^{(2)} \leq L_2 - 1. \quad (45)$$

Since (45) holds for all network setups, then the following APD-related design criterion must be considered.

Criterion *3:* The asymptotic APD is minimized by setting $l_{\text{th}}^{(1)} = l_{\text{th}}^{(2)} = 0$ resulting in the minimum achievable APD value of $7/2$.

E. Conclusions and Future Work: Optimizing the BA two-way relaying scheme

Following from the asymptotic design criteria that were reached, the following conclusions can be made regarding the design of the DF BA two-way relaying systems.

- Regarding the threshold levels $l_{\text{th}}^{(1)}$ and $l_{\text{th}}^{(2)}$, the best choice corresponds to setting $l_{\text{th}}^{(1)} = l_{\text{th}}^{(2)} = 0$. This choice minimizes the asymptotic APD (following from criterion 3) whereas any other choice will increase the APD without offering any additional advantage in terms of the asymptotic OP or diversity order (following from criterion 1 and criterion 2).
- Regarding the buffer sizes L_1 and L_2, the following conclusions can be reached by fixing $l_{\text{th}}^{(1)} = l_{\text{th}}^{(2)} = 0$ in criterion 1 and criterion 2:
  - Setting $L_1 = 3$ and $L_2 = 3$ achieves the maximum diversity order with the highest coding gain for any network setup.
  - Increasing L_1 and/or L_2 beyond 3 does not present any particular advantage for high values of the SNR.
  - Smaller buffers can be used depending on the network setup as follows. (i): For $\mu_1 < \mu_2$, selecting $(L_1, L_2) = (2, 3)$ still achieves the maximum diversity order at the expense of a reduced coding gain compared to the choice $(L_1, L_2) = (3, 3)$. (ii): For $\mu_1 > \mu_2$, a similar conclusion can be reached by selecting $(L_1, L_2) = (3, 2)$. (iii): For $\mu_1 = \mu_2 = \mu$, the choices $(L_1, L_2) \in \{(2, 3), (3, 2), (2, 2)\}$ are all feasible in the sense of maximizing the diversity order. In this case, the smallest buffer sizes choice of $(L_1, L_2) = (2, 2)$ suffers from the smallest coding gain. Moreover, from (39), the choice $(L_1, L_2) = (2, 3)$ will result in a higher coding gain than the choice $(L_1, L_2) = (3, 2)$ if $\frac{a_2}{a_1} > \left(\frac{b_2}{b_1}\right)^{\mu}$ since $\beta_2 = \beta_4 = \frac{2}{3}$ for $l_{\text{th}}^{(1)} = l_{\text{th}}^{(2)}$ following from Table I.

The main challenge in generalizing the proposed scheme and associated formulation to the multi-relay scenario resides in the complexity of the Markov chain analysis. In fact, for a K relay network, the Markov chain will involve $(L_1+1)^K(L_2+1)^K$ states implying an exponential increase in the number of states. Moreover, the joint relay-selection/mode-selection optimization problem will involve $2K$ threshold levels that can assume $(L_1 L_2)^K$ possible values. While our work considered the single-relay case as in [13]–[21], we hope that this work will motivate more research in the direction of proposing efficient multi-relay two-way cooperative schemes. In addition to extending the proposed scheme to the multi-relay scenario, future work must tackle the issue of energy harvesting for the sake of enhancing the energy efficiency.

V. NUMERICAL RESULTS

We next present some numerical results that support the theoretical findings reported in the previous sections. The numerical results were obtained by running ten million Monte Carlo simulations that yielded accurate OP and APD results for the SNR values that are not very large. We denote by d_1 the distance between A and R and by d_2 the distance between B and R. We assume that the relay is placed along the line joining A with B implying that the distance between A and B is equal to $d_1 + d_2$. The parameters of the $\kappa-\mu$ distribution are taken to be distance dependent with $(\kappa_i, \mu_i) = (\kappa(d_i), \mu(d_i))$ for $i = 1$ (A-R link) and $i = 2$ (B-R link). We consider link distances of 1 km and 2 km and assume that $\kappa(1) = 1.5$ and $\mu(1) = 3$ whereas $\kappa(2) = 1.25$ and $\mu(2) = 2$. Assuming a power loss exponent of 2, the $\Omega_i = \left(\frac{d_1+d_2}{d_i}\right)^2$ for $i = 1, 2$ in (1)-(2) [23]. Finally, we consider a target rate of $r_0 = 1$ BPCU.

A. Effect of the Threshold Levels

Fig. 2 and Fig. 3 highlight the impact of the threshold parameters $l_{\text{th}}^{(1)}$ and $l_{\text{th}}^{(2)}$ on the OP and APD, respectively.

TABLE III
ASYMPTOTIC VALUES OF THE OUTAGE PROBABILITY

	$l_{\text{th}}^{(2)} < L_2 - 2$	$l_{\text{th}}^{(2)} = L_2 - 2$	$l_{\text{th}}^{(2)} = L_2 - 1$
$l_{\text{th}}^{(1)} < L_1 - 2$	pq	$pq + \beta_4 p^2$	$pq + \beta_3 p$
$l_{\text{th}}^{(1)} = L_1 - 2$	$pq + \beta_2 q^2$	$pq + \beta_2 q^2 + \beta_4 p^2$	$pq + \beta_2 q^2 + \beta_3 p$
$l_{\text{th}}^{(1)} = L_1 - 1$	$pq + \beta_1 q$	$pq + \beta_1 q + \beta_4 p^2$	$pq + \beta_1 q + \beta_3 p$

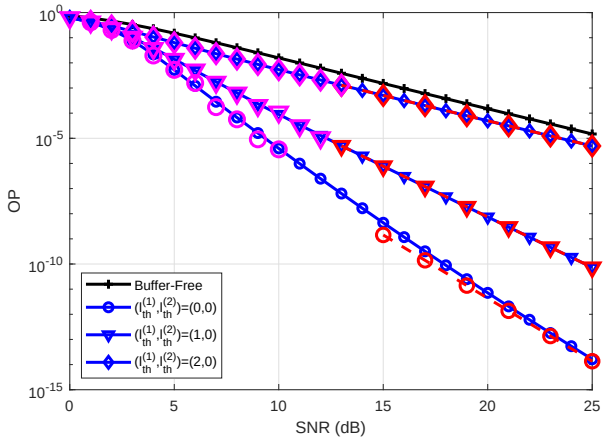

Fig. 2. Outage Probability for $d_1 = 1$ km and $d_2 = 2$ km and $L_1 = L_2 = 3$. Solid and dashed lines correspond to the exact and asymptotic values (from Table III), respectively. Markers without lines correspond to the simulation values.

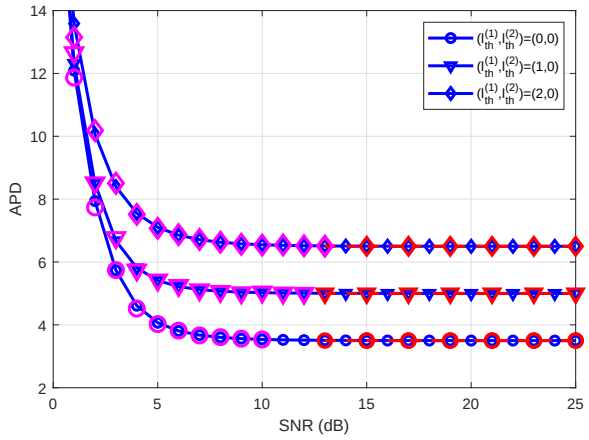

Fig. 3. Average Packet Delay for $d_1 = 1$ km and $d_2 = 2$ km and $L_1 = L_2 = 3$. Solid and dashed lines correspond to the exact and asymptotic values (from (45)), respectively. Markers without lines correspond to the simulation values.

We fix $L_1 = L_2 = 3$ and $(d_1, d_2) = (1, 2)$ km (resulting in $\mu_1 = 3$ and $\mu_2 = 2$). We consider the three cases $(l_{\text{th}}^{(1)}, l_{\text{th}}^{(2)}) \in \{(0,0), (1,0), (2,0)\}$. Since $\mu_1 > \mu_2$ in this simulation setup, then only the choice $(l_{\text{th}}^{(1)}, l_{\text{th}}^{(2)}) = (0,0)$ will achieve the maximum diversity order as highlighted in criterion 2. This observation is demonstrated in Fig. 2 where the highest diversity order (steepest OP curve) is obtained for $(l_{\text{th}}^{(1)}, l_{\text{th}}^{(2)}) = (0,0)$. Results in Fig. 2 highlight on the accuracy of the asymptotic OP expressions provided in Table III in predicting the performance for average-to-large values of the SNR. In fact, a perfect overlap is observed between the exact and asymptotic OP curves for large values of the SNR. Moreover, results in Fig. 2 demonstrate the accuracy of the diversity orders provided in Table II. The three considered values of $(l_{\text{th}}^{(1)}, l_{\text{th}}^{(2)}) = (0,0)$, $(l_{\text{th}}^{(1)}, l_{\text{th}}^{(2)}) = (1,0)$ and $(l_{\text{th}}^{(1)}, l_{\text{th}}^{(2)}) = (2,0)$ correspond to the scenarios $\left[l_{\text{th}}^{(1)} < L_1 - 2 \; ; \; l_{\text{th}}^{(2)} < L_2 - 2\right]$, $\left[l_{\text{th}}^{(1)} = L_1 - 2 \; ; \; l_{\text{th}}^{(2)} < L_2 - 2\right]$ and $\left[l_{\text{th}}^{(1)} = L_1 - 1 \; ; \; l_{\text{th}}^{(2)} < L_2 - 2\right]$ that appear in the first column of Table II, respectively. The corresponding diversity orders are $\mu_1 + \mu_2 = 5$, $\mu_2 + \min\{\mu_1, \mu_2\} = 4$ and $\mu_2 = 2$, respectively, where all of these values are demonstrated in Fig. 2. Since the buffer-free (BF) system achieves a diversity order of $\min\{\mu_1, \mu_2\} = \mu_2$ in this simulation setup, then the choice $(l_{\text{th}}^{(1)}, l_{\text{th}}^{(2)}) = (2,0)$ is highly suboptimal since it does not result in any diversity gain compared to the conventional BF system. Since the asymptotic OP of the BF system is approximately q while the asymptotic OP of the BA system with $(l_{\text{th}}^{(1)}, l_{\text{th}}^{(2)}) = (2,0)$ is approximately $\beta_1 q = \frac{1}{3} q$ from Table III and Table I, then the only advantage of the latter system resides in a coding gain of $\frac{10}{\mu_2} \log_{10}(3) \approx 2.4$ dB. This theoretical coding gain matches the numerical value that can be obtained from Fig. 2. Finally, Fig. 3 shows the variation of the APD as a function of the SNR and demonstrates the accuracy of the asymptotic expression provided in (45). As a conclusion, the choice $(l_{\text{th}}^{(1)}, l_{\text{th}}^{(2)}) = (0,0)$ not only minimizes the OP, but it also minimizes the APD as highlighted in Fig. 3. In this simulation setup where $l_{\text{th}}^{(2)}$ is fixed to zero, increasing the value of $l_{\text{th}}^{(1)}$ by one will incur an increase of the asymptotic APD by 1.5 as highlighted in (45) and Fig. 3. Finally, results show that the theoretical curves almost perfectly overlap with the numerical curves in all simulated scenarios thus highlighting on the accuracy of the results. The usefulness of the theoretical analysis resides in its capability of providing accurate results for all SNR values while the numerical analysis is limited to small-to-average SNRs where prohibitively large numbers of iterations are not required for yielding accurate results. Since a close match between the theoretical and numerical results was observed in all simulation setups, the numerical results will not be shown in the subsequent figures for the sake of clarity.

B. Effect of the Buffer Sizes

In Fig. 4 and Fig. 5, we fix the threshold levels to their optimal values $l_{\text{th}}^{(1)} = l_{\text{th}}^{(2)} = 0$ and we consider the buffer sizes

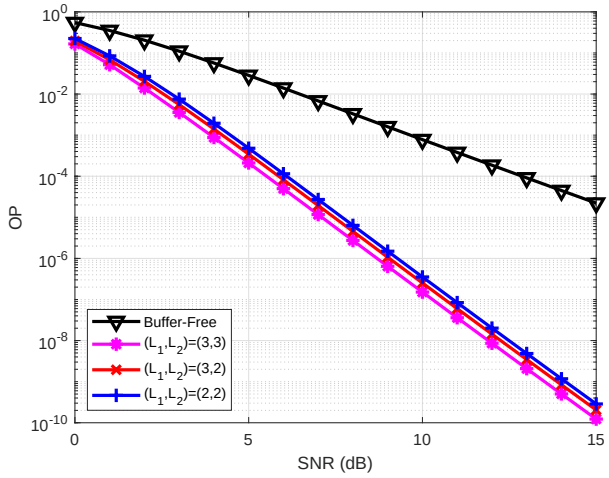

Fig. 4. Outage Probability for $d_1 = d_2 = 1$ km and $l_{\text{th}}^{(1)} = l_{\text{th}}^{(2)} = 0$.

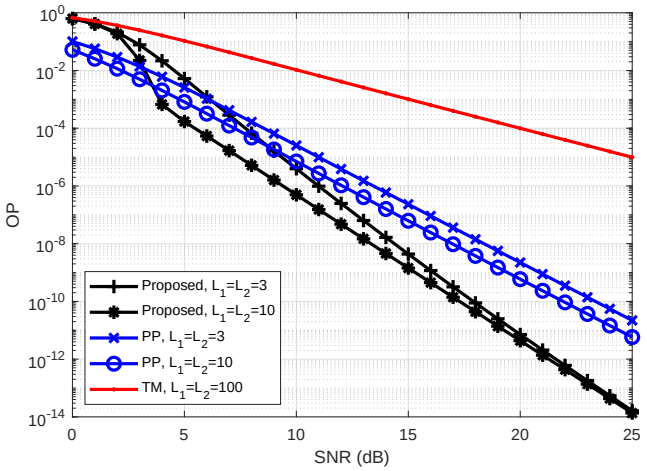

Fig. 6. Outage Probability of the proposed scheme versus the TM and PP schemes in [11] and [16], respectively.

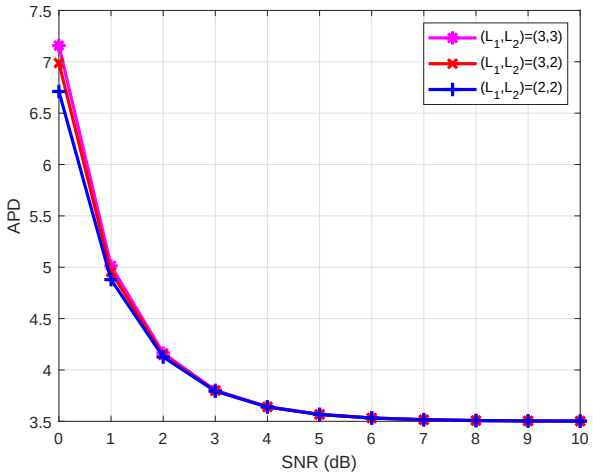

Fig. 5. Average Packet Delay for $d_1 = d_2 = 1$ km and $l_{\text{th}}^{(1)} = l_{\text{th}}^{(2)} = 0$.

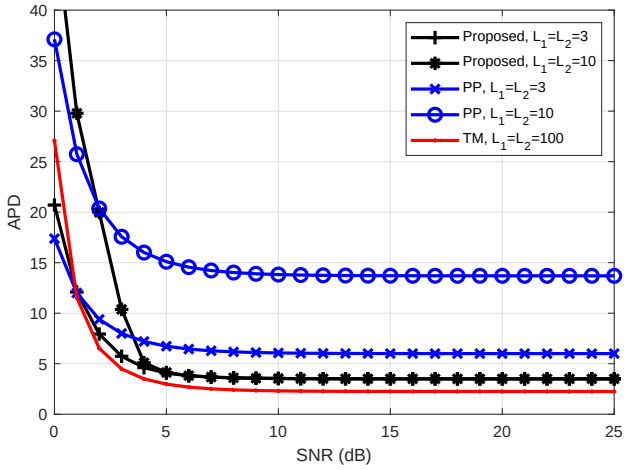

Fig. 7. Average Packet Delay of the proposed scheme versus the TM and PP schemes in [11] and [16], respectively.

$(L_1, L_2) \in \{(3,3),(3,2),(2,2)\}$ for $d_1 = d_2 = 1$ km. The asymptotic OP and APD expressions from Table III and (45) show a perfect match with their exact counterparts for large values of the SNR and, hence, only the exact expressions are shown for the sake of clarity. For this simulation setup where $\mu_1 = \mu_2$, all considered buffer sizes achieve the maximum diversity order following from criterion 2 and Section IV-E. Results in Fig. 4 demonstrate a diversity order of $\mu_1 + \mu_2 = 6$ where the different OP curves are parallel to each other for large values of the SNR. Results in Fig. 4 also highlight on the accuracy of (39) and show that the option $(L_1, L_2) = (3,3)$ (resp. $(L_1, L_2) = (2,2)$) shows the best (resp. worst) performance as predicated by the analytical derivations. Results in Fig. 4 show the huge performance gains that can be reaped through equipping the relay with buffers. For example, the BA scheme with $L_1 = L_2 = 3$ outperforms the BF system by around 7.4 dB for an OP value of 10^{-4}. Results in Fig. 5 highlight on the accuracy of the asymptotic APD value of 3.5 for all considered values of (L_1, L_2). In this regard, increasing the buffer sizes results in a slight increase in the APD for small values of the SNR without affecting the APD performance for average-to-large values of the SNR.

C. Comparison with the Existing Schemes

In what follows, we compare the proposed scheme with the existing BA two-way relaying schemes in [11], [15], [16]. The schemes in [15] achieve a diversity order of one over Rayleigh fading channels (refer to proposition 4, proposition 5 and proposition 7 in [15]). Therefore, the proposed scheme presents the predominant advantage of doubling the diversity order over such channels since $\mu_1 + \mu_2 = 2$ (with $\mu_1 = \mu_2 = 1$ over Rayleigh fading channels). As such, the schemes in [15] suffer from severe OP degradations especially for large values of the SNR. Moreover, in [15], while the deterministic approach for constraining the delay achieves constant asymptotic delays, the probabilistic approach incurs delays that increase with the buffer size unlike the proposed scheme where increasing the buffer size does not increase the delay.

In Fig. 6 and Fig. 7, the OP and APD of the proposed scheme (with $l_{\text{th}}^{(1)} = l_{\text{th}}^{(2)} = 0$) are compared with those of the throughput-maximizing (TM) scheme in [11] and the practical-protocol (PP) in [16]. In these figures, we fix $d_1 = 1$ km and $d_2 = 2$ km. For the proposed scheme, results in Fig. 6 and Fig. 7 demonstrate that the options $L_1 = L_2 = 3$ and $L_1 = L_2 = 10$ achieve the same OP and APD performance levels in the asymptotic SNR regime. For small values of the SNR, results show that increasing the buffer sizes results in a marginal decrease in the OP that comes at the expense of a noteworthy increase in the APD. Comparing the proposed scheme with [16] highlights on the superiority of the proposed optimized scheme in concurrently reducing the OP and APD for average-to-large values of the SNR. Unlike the proposed scheme where a buffer size of three is sufficient for attaining the best OP and APD performance asymptotically, results in Fig. 6 and Fig. 7 show that, for the scheme in [16], increasing the buffer size reduces the asymptotic OP at the expense of a significant increase in the asymptotic APD. Results in Fig. 7 are consistent with Lemma 1 in [16] that states that the asymptotic APD of this scheme increases with the buffer size unlike the proposed scheme. On the other hand, the scheme in [11] focuses on minimizing the end-to-end transmission time. As such, this scheme reduces the delay compared to the proposed scheme at the expense of suffering from excessively large OP values even with very large buffer sizes.

VI. Conclusion

We proposed and analyzed a novel threshold-based relaying scheme for BA two-way relaying systems. We studied the impact of the two threshold parameters on the diversity order, coding gain, outage probability and queuing delay and we suggested convenient choices of these parameters. The presented analytical framework was culminated by simple criteria for selecting the buffer sizes depending on the network topology. Results showed that small buffer sizes are sufficient for reaping the maximum performance gains at large SNR values.

Appendix A

We focus on the subset of states $\mathcal{S} = \{(l_{\text{th}}^{(1)}, l_{\text{th}}^{(2)}), (l_{\text{th}}^{(1)}+1, l_{\text{th}}^{(2)}), (l_{\text{th}}^{(1)}, l_{\text{th}}^{(2)}+1), (l_{\text{th}}^{(1)}+1, l_{\text{th}}^{(2)}+1)\}$ and we prove that this subset is closed for asymptotically large values of the SNR. In this context, the transition probability from any state inside $\mathcal{S}$ to any state outside $\mathcal{S}$ tends to zero. Consequently, after a certain number of iterations, the Markov chain will be in the states of $\mathcal{S}$ with a probability tending to one at steady-state: $\sum_{(l_1,l_2)\in\mathcal{S}} \pi_{l_1,l_2} \to 1$.

Consider first the state $(l_{\text{th}}^{(1)}+1, l_{\text{th}}^{(2)}+1)$ where the transition probabilities out of this state are provided in (7)-(10). For $p \to 0$ and $q \to 0$, (7) shows that:

$$t_{(l_{\text{th}}^{(1)}+1, l_{\text{th}}^{(2)}+1),(l_{\text{th}}^{(1)}, l_{\text{th}}^{(2)})} \to 1, \tag{46}$$

while (8)-(10) show that all remaining transition probabilities will tend to zero.

Considering the state $(l_{\text{th}}^{(1)}, l_{\text{th}}^{(2)}+1)$, (11)-(13) show that:

$$t_{(l_{\text{th}}^{(1)}, l_{\text{th}}^{(2)}+1),(l_{\text{th}}^{(1)}+1, l_{\text{th}}^{(2)}+1)} \to 1, \tag{47}$$

while all other transition probabilities will tend to zero.

Similarly, for the state $(l_{\text{th}}^{(1)}+1, l_{\text{th}}^{(2)})$, (14)-(16) show that all transition probabilities out of this state will tend to zero except for:

$$t_{(l_{\text{th}}^{(1)}+1, l_{\text{th}}^{(2)}),(l_{\text{th}}^{(1)}+1, l_{\text{th}}^{(2)}+1)} \to 1. \tag{48}$$

Finally, for the state $(l_{\text{th}}^{(1)}, l_{\text{th}}^{(2)})$, the transition probabilities will depend on whether $l_{\text{th}}^{(1)} < l_{\text{th}}^{(2)}$, $l_{\text{th}}^{(1)} > l_{\text{th}}^{(2)}$ or $l_{\text{th}}^{(1)} = l_{\text{th}}^{(2)}$ as highlighted in (18)-(19):

$$\begin{cases} \pi_{(l_{\text{th}}^{(1)}, l_{\text{th}}^{(2)}),(l_{\text{th}}^{(1)}+1, l_{\text{th}}^{(2)})} \to 1, & l_{\text{th}}^{(1)} < l_{\text{th}}^{(2)}; \\ \pi_{(l_{\text{th}}^{(1)}, l_{\text{th}}^{(2)}),(l_{\text{th}}^{(1)}, l_{\text{th}}^{(2)}+1)} \to 1, & l_{\text{th}}^{(1)} > l_{\text{th}}^{(2)}; \\ \begin{cases} \pi_{(l_{\text{th}}^{(1)}, l_{\text{th}}^{(2)}),(l_{\text{th}}^{(1)}+1, l_{\text{th}}^{(2)})} \to \frac{1}{2}, \\ \pi_{(l_{\text{th}}^{(1)}, l_{\text{th}}^{(2)}),(l_{\text{th}}^{(1)}, l_{\text{th}}^{(2)}+1)} \to \frac{1}{2}, \end{cases} & l_{\text{th}}^{(1)} = l_{\text{th}}^{(2)}. \end{cases} \tag{49}$$

After deriving the transition probabilities among the states of $\mathcal{S}$ according to (46)-(49), the steady-state probabilities of these states can be obtained by solving the balance equations subject to $\sum_{(l_1,l_2)\in\mathcal{S}} \pi_{l_1,l_2} = 1$. For $l_{\text{th}}^{(1)} < l_{\text{th}}^{(2)}$, these equations are given by $\pi_{l_{\text{th}}^{(1)}, l_{\text{th}}^{(2)}} = \pi_{l_{\text{th}}^{(1)}+1, l_{\text{th}}^{(2)}+1}$, $\pi_{l_{\text{th}}^{(1)}+1, l_{\text{th}}^{(2)}} = \pi_{l_{\text{th}}^{(1)}, l_{\text{th}}^{(2)}}$, $\pi_{l_{\text{th}}^{(1)}+1, l_{\text{th}}^{(2)}+1} = \pi_{l_{\text{th}}^{(1)}+1, l_{\text{th}}^{(2)}}$ and $\pi_{l_{\text{th}}^{(1)}, l_{\text{th}}^{(2)}+1} = 0$. The solution of these equations results in the matrix $\mathbf{M}_1^{(0)}$ in (33). Similarly, for $l_{\text{th}}^{(1)} > l_{\text{th}}^{(2)}$, solving the equations $\pi_{l_{\text{th}}^{(1)}, l_{\text{th}}^{(2)}} = \pi_{l_{\text{th}}^{(1)}+1, l_{\text{th}}^{(2)}+1}$, $\pi_{l_{\text{th}}^{(1)}, l_{\text{th}}^{(2)}+1} = \pi_{l_{\text{th}}^{(1)}, l_{\text{th}}^{(2)}}$, $\pi_{l_{\text{th}}^{(1)}+1, l_{\text{th}}^{(2)}+1} = \pi_{l_{\text{th}}^{(1)}, l_{\text{th}}^{(2)}+1}$ and $\pi_{l_{\text{th}}^{(1)}+1, l_{\text{th}}^{(2)}} = 0$ results in the matrix $\mathbf{M}_2^{(0)}$ in (33). Finally, for $l_{\text{th}}^{(1)} = l_{\text{th}}^{(2)}$, the balance equations are given by $\pi_{l_{\text{th}}^{(1)}, l_{\text{th}}^{(2)}} = \pi_{l_{\text{th}}^{(1)}+1, l_{\text{th}}^{(2)}+1}$, $\pi_{l_{\text{th}}^{(1)}+1, l_{\text{th}}^{(2)}} = \frac{1}{2}\pi_{l_{\text{th}}^{(1)}, l_{\text{th}}^{(2)}}$, $\pi_{l_{\text{th}}^{(1)}, l_{\text{th}}^{(2)}+1} = \frac{1}{2}\pi_{l_{\text{th}}^{(1)}, l_{\text{th}}^{(2)}}$ and $\pi_{l_{\text{th}}^{(1)}+1, l_{\text{th}}^{(2)}+1} = \pi_{l_{\text{th}}^{(1)}+1, l_{\text{th}}^{(2)}} + \pi_{l_{\text{th}}^{(1)}, l_{\text{th}}^{(2)}+1}$ whose solution results in the matrix $\mathbf{M}_3^{(0)}$ in (33).

Appendix B

The steady-state probabilities can be written under the general form $\pi_{l_1,l_2} = \sum_{i\geq 0}\sum_{j\geq 0} k_{i,j} p^i q^j$ where $\{k_{i,j}\}$ are constants. We define the asymptotic order of the probability π_{l_1,l_2} as:

$$O(\pi_{l_1,l_2}) = \min_{i\geq 0\ ;\ j\geq 0} \{i+j \ \mid \ k_{i,j} = 0 \ \forall \ i+j < O(\pi_{l_1,l_2})\}. \tag{50}$$

For example, $O(1/3 - p + q + \cdots) = 0$ and $O(p^2 + pq + \cdots) = 2$. Since this appendix revolves around an order-1 asymptotic analysis, then we assume that $\pi_{l_1,l_2} \to 0$ whenever $O(\pi_{l_1,l_2}) \geq 2$.

We fix $m \triangleq l_{\text{th}}^{(1)}$ and $n \triangleq l_{\text{th}}^{(2)}$ for notational simplicity. We focus on the following subset of nine states for $m \leq L_1 - 2$ and $n \leq L_2 - 2$:

$$\mathcal{S} = \{(m+i, n+j)\ ;\ i,j = 0,1,2\} \triangleq \mathcal{S}_1 \cup \mathcal{S}_2, \tag{51}$$

where:

$$\mathcal{S}_1 = \{(m,n), (m,n+1), (m+1,n), (m+1,n+1)\} \tag{52}$$

$$\mathcal{S}_2 = \{(m+2,n), (m+2,n+1), (m,n+2), (m+1,n+2), (m+2,n+2)\}. \tag{53}$$

By definition, a subset of states is declared to be *closed* if the probability of leaving this subset is equal to zero. Similarly, a subset of states is declared to be *quasi-closed* if the probability of leaving this subset is small. The reason behind focusing on the subset $\mathcal{S}$ in (51) is justified by the following proposition.

Proposition *3:* The subset $\mathcal{S}$ in (51) is asymptotically closed for $m = L_1 - 2$ and $n = L_2 - 2$ and it is asymptotically quasi-closed otherwise.

Proof: We denote by $\mathcal{T}_{l_1,l_2}$ as the set of states that can be reached from the state (l_1, l_2) (excluding the state (l_1, l_2) itself).

We first consider the subset $\mathcal{S}_1$. (i): From (17)-(19), $\mathcal{T}_{m,n} = \{(m+1, n), (m, n+1)\}$. (ii): From (11)-(13), $\mathcal{T}_{m,n+1} = \{(m+1, n+1), (m, n+2)\}$. (iii): From (14)-(16), $\mathcal{T}_{m+1,n} = \{(m+1, n+1), (m+2, n)\}$. (iv): Finally, from (7)-(10), $\mathcal{T}_{m+1,n+1} = \{(m, n), (m+1, n+2), (m+2, n+1)\}$. Consequently, we cannot leave the set $\mathcal{S}$ from any of the four states in $\mathcal{S}_1$.

Next, we consider the states in $\mathcal{S}_2$ for which the set $\mathcal{T}_{m+i,n+j}$ can be partitioned as follows:

$$\mathcal{T}_{m+i,n+j} = \mathcal{T}^{(0)}_{m+i,n+j} \cup \left\{ \begin{array}{ll} \mathcal{T}^{(1)}_{m+i,n+j}, & m < L_1 - 2; \\ \phi, & m = L_1 - 2. \end{array} \right. \cup \left\{ \begin{array}{ll} \mathcal{T}^{(2)}_{m+i,n+j}, & n < L_2 - 2; \\ \phi, & n = L_2 - 2. \end{array} \right. , \quad (54)$$

where ϕ denotes the empty set. While the set $\mathcal{T}^{(0)}_{m+i,n+j}$ is included in $\mathcal{S}$, the sets $\mathcal{T}^{(1)}_{m+i,n+j}$ and $\mathcal{T}^{(2)}_{m+i,n+j}$ are not included in $\mathcal{S}$.

(v): From (14)-(16), $\mathcal{T}^{(0)}_{m+2,n} = \{(m+2, n+1)\}$, $\mathcal{T}^{(1)}_{m+2,n} = \{(m+3, n)\}$ and $\mathcal{T}^{(2)}_{m+2,n} = \phi$. (vi): From (7)-(10), $\mathcal{T}^{(0)}_{m+2,n+1} = \{(m+1, n), (m+2, n+2)\}$, $\mathcal{T}^{(1)}_{m+2,n+1} = \{(m+3, n+1)\}$ and $\mathcal{T}^{(2)}_{m+2,n+1} = \phi$. (vii): From (11)-(13), $\mathcal{T}^{(0)}_{m,n+2} = \{(m+1, n+2)\}$, $\mathcal{T}^{(1)}_{m,n+2} = \phi$ and $\mathcal{T}^{(2)}_{m,n+2} = \{(m, n+3)\}$. (viii): From (7)-(10), $\mathcal{T}^{(0)}_{m+1,n+2} = \{(m+2, n+2), (m, n+1)\}$, $\mathcal{T}^{(1)}_{m+1,n+2} = \phi$ and $\mathcal{T}^{(2)}_{m+1,n+2} = \{(m+1, n+3)\}$. (ix): Finally, from (7)-(10), $\mathcal{T}^{(0)}_{m+2,n+2} = \{(m+1, n+1)\}$, $\mathcal{T}^{(1)}_{m+2,n+2} = \{(m+3, n+2)\}$ and $\mathcal{T}^{(2)}_{m+2,n+2} = \{(m+2, n+3)\}$.

From (54), for $m = L_1 - 2$ and $n = L_2 - 2$, $\mathcal{T}_{m+i,n+j} = \mathcal{T}^{(0)}_{m+i,n+j} \subset \mathcal{S}$ implying that we cannot leave the set $\mathcal{S}$ from any of the five states in $\mathcal{S}_2$. As such, the set $\mathcal{S} = \mathcal{S}_1 \cup \mathcal{S}_2$ is closed.

On the other hand, when $m < L_1 - 2$ or $n < L_2 - 2$, the states in $\mathcal{S}_2$ might lead to states outside $\mathcal{S}$ since $\mathcal{T}^{(1)}_{m+i,n+j} \cup \mathcal{T}^{(2)}_{m+i,n+j} \not\subset \mathcal{S}$. However, the corresponding transition probabilities are small for large values of the SNR. In fact, $t_{(m+i,n+2),(m+i,n+3)} = p \ll 1$ for $i = 0, 1, 2$ and $t_{(m+2,n+j),(m+3,n+j)} = q \ll 1$ for $j = 0, 1, 2$ following from (7)-(19). Therefore, as the probability of exiting $\mathcal{S}$ from the states in $\mathcal{S}_1$ is zero while the probability of exiting $\mathcal{S}$ from the states in $\mathcal{S}_2$ is in the order of p or q that are both very small for large values of the SNR, then the subset $\mathcal{S}$ will be quasi-closed in this case. ■

The relative values of m and n will only affect the transition probabilities from the state (m, n) as highlighted in (18)-(19).

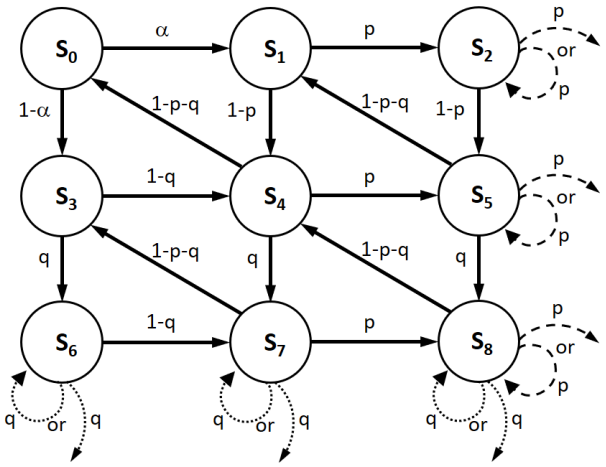

Fig. 8. Transitions among the states of the set $\mathcal{S}$ where the probability α is defined in (55). The self-loops of transition probability p (resp. q) at the states S_2, S_5 and S_8 (resp. S_6, S_7 and S_8) exist if $l^{(2)}_{\text{th}} = L_2 - 2$ (resp. $l^{(1)}_{\text{th}} = L_1 - 2$).

We denote $t_{(m,n),(m,n+1)} = 1 - t_{(m,n),(m+1,n)} \triangleq \alpha$ where:

$$\alpha = \left\{ \begin{array}{ll} p, & l^{(1)}_{\text{th}} < l^{(2)}_{\text{th}}; \\ 1 - q, & l^{(1)}_{\text{th}} > l^{(2)}_{\text{th}}; \\ \frac{1+p-q}{2}, & l^{(1)}_{\text{th}} = l^{(2)}_{\text{th}}. \end{array} \right. . \quad (55)$$

The state diagram describing the transitions between the states of $\mathcal{S}$ is provided in Fig. 8. For simplicity of notation, the states will be numbered as $S_0 = (m, n)$, $S_1 = (m, n+1)$, $S_2 = (m, n+2)$, $S_3 = (m+1, n)$, $S_4 = (m+1, n+1)$, $S_5 = (m+1, n+2)$, $S_6 = (m+2, n)$, $S_7 = (m+2, n+1)$ and $S_8 = (m+2, n+2)$. Moreover, the steady-state probability of the state S_i will be denoted by π_i for $i = 0, \ldots, 8$.

From Fig. 8, the balance equations at states S_0, S_3 and S_6 are given by:

$$\pi_0 = (1 - p - q)\pi_4 \quad (56)$$

$$\pi_3 = (1 - \alpha)\pi_0 + (1 - p - q)\pi_7 \quad (57)$$

$$(1 - q')\pi_6 = q\pi_3, \quad (58)$$

where $q' = q$ if $m = L_1 - 2$ and $q' = 0$ if $m < L_1 - 2$. Introducing the probability q' in (58) accounts for the self-loop at the state S_6 when $m = L_1 - 2$ and for the transition from this state to the state $(m + 3, n)$ when $m < L_1 - 2$.

Similarly, from Fig. 8, the balance equations at states S_1, S_4 and S_7 are given by:

$$\pi_1 = \alpha\pi_0 + (1 - p - q)\pi_5 \quad (59)$$

$$\pi_4 = (1 - q)\pi_3 + (1 - p)\pi_1 + (1 - p - q)\pi_8 \quad (60)$$

$$(1 - q')\pi_7 = q\pi_4 + (1 - q)\pi_6. \quad (61)$$

Finally, at states S_2, S_5 and S_8:

$$(1 - p')\pi_2 = p\pi_1 \quad (62)$$

$$(1 - p')\pi_5 = p\pi_4 + (1 - p)\pi_2 \quad (63)$$

$$(1 - p' - q')\pi_8 = p\pi_7 + q\pi_5, \quad (64)$$

where $p' = p$ if $n = L_2 - 2$ and $p' = 0$ if $n < L_2 - 2$.

From (61), $O(\pi_7) \geq 1$ following from the multiplication of π_4 by q. Similarly, from (63), $O(\pi_5) \geq 1$. Now, since $O(\pi_7) \geq 1$ and $O(\pi_5) \geq 1$, then $O(\pi_8) \geq 2$ following from (64). Consequently, $\pi_8 = 0$ when performing the order-1 asymptotic analysis.

In the asymptotic regime, (56)-(58) can be further simplified as follows:

$$\pi_0 = (1-p-q)\pi_4 \ ; \ \pi_3 = (1-\alpha)\pi_0+\pi_7 \ ; \ \pi_6 = q\pi_3, \quad (65)$$

where the second equation follows since $(1-p-q)\pi_7 \approx \pi_7$ since $O(p\pi_7) = O(q\pi_7) \geq 2$ following from the fact that $O(\pi_7) \geq 1$. The last equation follows since $\frac{q}{1-q'} \approx q+qq' \approx q$ since either $O(qq') = O(q^2) = 2$ (for $m = L_1 - 2$) or $qq' = 0$ otherwise.

Similarly, for an order-1 asymptotic analysis, (59)-(61) can be simplified as follows:

$$\pi_1 = \alpha\pi_0+\pi_5 \ ; \ \pi_4 = (1-q)\pi_3+(1-p)\pi_1 \ ; \ \pi_7 = q\pi_4+\pi_6, \quad (66)$$

where the first equation follows since $(1-p-q)\pi_5 \approx \pi_5$ since $O(\pi_5) \geq 1$, the second equation follows from replacing $\pi_8 = 8$ while the last equation follows since $O(1-q') = 0$ for $q' = q$ or $q' = 0$ while $(1-q)\pi_6 \approx \pi_6$ since $O(\pi_6) \geq 1$ following from the last equation in (65).

Carrying out similar simplifications, (62)-(63) can be written as:

$$\pi_2 = p\pi_1 \ \ ; \ \ \pi_5 = p\pi_4 + (1-p)\pi_2. \quad (67)$$

Manipulating equations (65)-(67) while ignoring the high order terms shows that the probabilities $\{\pi_i \ ; \ i = 0, 1, 2, 3, 5, 6, 7\}$ can be related to the probability π_4 as follows. (i): $\pi_0 = (1-p-q)\pi_4$. (ii): $\pi_1 = [\alpha+(1-\alpha)p-\alpha q]\pi_4$. (iii): $\pi_2 = \alpha p\pi_4$. (iv): $\pi_3 = [1-\alpha-(1-\alpha)p+q]\pi_4$. (v): $\pi_5 = (1+\alpha)p\pi_4$. (vi): $\pi_6 = (1-\alpha)q\pi_4$. (vii): $\pi_7 = (2-\alpha)q\pi_4$. Replacing these probabilities in the equation $\sum_{i=0}^{8} \pi_i = 1$ and solving for π_4 results in:

$$\pi_4 = \frac{1}{3 + 2\alpha p + 3(1-\alpha)q}. \quad (68)$$

For $l_{\text{th}}^{(1)} < l_{\text{th}}^{(2)}$, replacing α by p in (68) results in $\pi_4 = \frac{1-q}{3}$. For $l_{\text{th}}^{(1)} > l_{\text{th}}^{(2)}$ and $l_{\text{th}}^{(1)} = l_{\text{th}}^{(2)}$, replacing α by $1-q$ and $\frac{1+p-q}{2}$ in (68) results in $\pi_4 = \frac{1}{3} - \frac{2p}{9}$ and $\pi_4 = \frac{1}{3} - \frac{p}{9} - \frac{q}{6}$, respectively. Replacing in the equations that relate the different probabilities to π_4 results in the matrices $\mathbf{M}_1^{(1)}$, $\mathbf{M}_2^{(1)}$ and $\mathbf{M}_3^{(1)}$ in (36), respectively.

REFERENCES

[1] N. Nomikos, T. Charalambous, I. Krikidis, D. N. Skoutas, D. Vouyioukas, M. Johansson, and C. Skianis, "A survey on buffer-aided relay selection," *IEEE Commun. Surveys & Tutorials*, vol. 18, no. 2, pp. 1073–1097, Dec. 2015.

[2] R. Kumar and A. Hossain, "Survey on half-and full-duplex relay based cooperative communications and its potential challenges and open issues using Markov chains," *IET Communications*, vol. 13, no. 11, pp. 1537–1550, May 2019.

[3] I. Krikidis, T. Charalambous, and J. S. Thompson, "Buffer-aided relay selection for cooperative diversity systems without delay constraints," *IEEE Trans. Wireless Commun.*, vol. 11, no. 5, pp. 1957–1967, May 2012.

[4] S. Luo and K. C. Teh, "Buffer state based relay selection for buffer-aided cooperative relaying systems," *IEEE Trans. Wireless Commun.*, vol. 14, no. 10, pp. 5430–5439, Oct. 2015.

[5] Z. Tian, Y. Gong, G. Chen, and J. Chambers, "Buffer-aided relay selection with reduced packet delay in cooperative networks," *IEEE Trans. Veh. Technol.*, vol. 66, no. 3, pp. 2567–2575, Mar. 2017.

[6] C. Abou-Rjeily, "Toward a better comprehension of decode-and-forward buffer-aided relaying: Case study of a single relay," *IEEE Commun. Lett.*, vol. 24, no. 5, pp. 1005–1009, May 2020.

[7] N. Zlatanov and R. Schober, "Buffer-aided relaying with adaptive link selection–fixed and mixed rate transmission," *IEEE Trans. Inform. Theory*, vol. 59, no. 5, pp. 2816–2840, May 2013.

[8] P. Xu, Z. Yang, Z. Ding, I. Krikidis, and Q. Chen, "A novel probabilistic buffer-aided relay selection scheme in cooperative networks," *IEEE Trans. Veh. Technol.*, vol. 69, no. 4, pp. 4548–4552, Apr. 2020.

[9] P. Xu, G. Chen, Z. Yang, and H. Lei, "Buffer-state-based probabilistic relay selection for cooperative networks with delay constraints," *IEEE Wireless Commun. Letters*, vol. PP, no. 99, 2020.

[10] H. Liu, P. Popovski, E. De Carvalho, and Y. Zhao, "Sum-rate optimization in a two-way relay network with buffering," *IEEE Commun. Lett.*, vol. 17, no. 1, pp. 95–98, Jan. 2013.

[11] L. Ding, M. Tao, F. Yang, and W. Zhang, "Joint scheduling and relay selection in one-and two-way relay networks with buffering," in *2009 IEEE Int. Conf. on Commun.* IEEE, 2009, pp. 1–5.

[12] H. Wang and B. Yang, "A new residual energy based relay selection in two-way buffer-aided relay networks," in *2017 Int. Conf. on Network and Information Systems for Computers (ICNISC)*, 2017, pp. 72–76.

[13] V. Jamali, N. Zlatanov, A. Ikhlef, and R. Schober, "Achievable rate region of the bidirectional buffer-aided relay channel with block fading," *IEEE Trans. Inform. Theory*, vol. 60, no. 11, pp. 7090–7111, Nov. 2014.

[14] V. Jamali, N. Zlatanov, and R. Schober, "Bidirectional buffer-aided relay networks with fixed rate transmission– Part I: Delay-unconstrained case," *IEEE Trans. Wireless Commun.*, vol. 14, no. 3, pp. 1323–1338, Mar. 2015.

[15] ——, "Bidirectional buffer-aided relay networks with fixed rate transmission–Part II: Delay-constrained case," *IEEE Trans. Wireless Commun.*, vol. 14, no. 3, pp. 1339–1355, Mar. 2015.

[16] S. Shi, S. Li, and J. Tian, "Markov modeling for practical two-way relay with finite relay buffers," *IEEE Commun. Lett.*, vol. 20, no. 4, pp. 768–771, April 2016.

[17] R. Liu, P. Popovski, and G. Wang, "Decoupled uplink and downlink in a wireless system with buffer-aided relaying," *IEEE Trans. Commun.*, vol. 65, no. 4, pp. 1507–1517, Apr. 2017.

[18] S. Luo and K. C. Teh, "Amplify-and-forward based two-way relay ARQ system with relay combination," *IEEE Commun. Lett.*, vol. 19, no. 2, pp. 299–302, Feb. 2014.

[19] J. Liu, M. Tao, and Y. Xu, "Alternative awaiting and broadcast for two-way relay fading channels," *IEEE Trans. Veh. Technol.*, vol. 62, no. 6, pp. 2841–2846, July 2013.

[20] S. Shi, W. Ni, and R. P. Liu, "Performance analysis of XOR two-way relay with finite buffers and instant scheduling," *IET Commun.*, vol. 11, no. 4, pp. 507–513, Mar. 2017.

[21] W. Ni, J. A. Zhang, Z. Fang, M. Abolhasan, R. P. Liu, and Y. J. Guo, "Analysis of finite buffer in two-way relay: a queueing theoretic point of view," *IEEE Trans. Veh. Technol.*, vol. 67, no. 4, pp. 3690–3694, Nov. 2017.

[22] X. Xie and X. Zhang, "Does full-duplex double the capacity of wireless networks?" in *IEEE INFOCOM IEEE Conference on Computer Communications*, 2014, pp. 253–261.

[23] D. Dixit and P. Sahu, "Exact closed-form ABER for multi-hop regenerative relay systems over $\kappa - \mu$ fading," vol. 6, no. 2, pp. 246–249, April 2017.

[24] J. D. C. Little and S. C. Graves, "Little's law," in *International Series in Operations Research & Management Science*, New York, NY, USA: Springer-Verlag, vol. 115, pp. 81–100, 2008.

[25] C. Abou-Rjeily and W. Fawaz, "Buffer-aided relaying protocols for cooperative FSO communications," *IEEE Trans. Wireless Commun.*, vol. 16, no. 12, pp. 8205–8219, Dec. 2017.